I. THE EFFECT OF PRESSURE ON THE INFRA-RED ABSORPTION OF OZONE

and

II. AN "ULTRA-SPECTROMETER" TECHNIQUE FOR INFRA-RED BANDS

Thesis

by

Martin Summerfield

In Partial Fulfillment of the Requirements for the Degree of Doctor of Philosophy

CALIFORNIA INSTITUTE OF TECHNOLOGY

Pasadena, California 1941

TABLE OF CONTENTS

ACKNOWLEDGEMENT

I would like to thank all those people who helped make this thesis possible. In particular, I am grateful to Dr. I. S. Bowen for his continued encouragement and interest, to Dr. W. Elsasser for many valuable discussions, and especially to Dr. John D. Strong, who not only suggested and guided this work, but by his contagious enthusiasm encouraged my love for research.

SUMMARY AND INTRODUCTION

In the course of developing a method for determining the height of the atmospheric ozone layer, it became necessary to determine the effect of total pressure on the absorption of radiation by the ozone band at 9.6μ. Accordingly, the transmission of ozone was measured with a reststrahlen receiver whose response curve was centered near 9.6μ. This was done at seven pressures between 6 mm. and 722 mm. with ozone thicknesses ranging up to 5 mm.

The proportionality of absorption to the square root of the thickness at low pressures suggested that the mechanism was Lorentz broadening. The possibility of using the dependence of band absorption on thickness as an ultra-spectrometer technique made it desirable to repeat the measurements with spectral resolution.

With these experimental results, it was found possible to deduce a value of the effective spacing of the lines in the band, and in this way a "line-density contour" of the ozone 9.6μ band was obtained. This density contour indicated that the band had a central branch, which served to strengthen the isosceles triangle model of the ozone molecule.

The name "ultra-spectrometer" was adopted to emphasize that the technique yields the spacing of the lines in a band when that spacing is far smaller than the available spectral resolving power. It was suggested by analogy with the ultra-microscope, an instrument that detects particles smaller than the available optical resolving power.

The importance of this technique as an aid in the identification of band types is readily appreciated when it is realized that all molecules but the simplest possess spectra unresolvable by present-day spectrometers. Without adequate resolving power it is difficult to deduce the rotational structure of a band, and unless this is known, it is impossible to assign the bands in a spectrum to specific vibrational modes. Hence, a "line-density contour" obtained with the ultra-spectrometer method may be decisive in the analysis of an infra-red spectrum.

I. EFFECT OF PRESSURE ON INFRA-RED ABSORPTION OF OZONE

1. On the Broadening of Spectral Lines.

The effect of pressure on infra-red band absorption is a result of the influence of pressure on the widths of the individual spectral lines. The status of present-day knowledge of the broadening of spectral lines is covered in the recent review by Margenau and Watson[1] from which the following remarks are taken.

The width of spectral lines can be attributed to combinations of the following factors:

1. Radiation damping.
2. Doppler effect.
3. Resonance broadening.
4. Broadening by forces of Van der Waals type.
5. Broadening by molecules with permanent electric fields.
6. Lorentz broadening.

To determine which of these types is applicable to the broadening of the ozone lines, we have to examine these widths quantitatively.

The first type, the so-called natural line width, depends only on the electromagnetic field of the isolated molecule and hence is independent of pressure. It is quite small for transitions obeying the usual selection rules, being of the order of 10^{-6} cm.$^{-1}$ in the band being

investigated.

The Doppler effect, at ordinary temperatures, results in a width of about 10^{-3} cm.$^{-1}$ in the region of 10μ, smaller by about one-half than the Lorentz width at the lowest pressure, 6 mm. Strictly speaking, the Doppler width is not negligible. However, the Doppler distribution is a very close one, and even when it exceeds the other types in width, it can be neglected in the wings of the lines. In our application, the relation between absorption and thickness of ozone is dependent almost exclusively on the shape of the wings of the lines. Therefore, it is not surprising that this relation, at 6 mm. pressure, is in agreement with the Lorentz type. (See Section 4.).

Resonance broadening is due to the interaction between similar molecules: in this case, the mutual effect of neighboring ozone molecules. It would be expected that the degree to which the line width is attributable to resonance effects would be dependent on the concentration of ozone in the ozone-oxygen mixture. The highest concentration used was about 40%, while the most important results are derived from the measurements on concentrations below 15%. Further, according to Margenau and Watson (loc. cit. p.40) the interactions between like molecules generally seem to affect infra-red lines in about the same manner as interactions between unlike molecules. There was no experimental evidence for any anomalous behavior in the ozone-ozone interaction, in these experiments.

We will, therefore, neglect resonance broadening.

Broadening due to the close proximity of foreign molecules carrying no permanent polar fields is called Van der Waals broadening. In general, it results in considerable line asymmetry because of actual alteration of the energy levels during the close collision. This type is dependent on the square of the gas density and does not become comparable with Lorentz broadening until high densities (several atmospheres pressure) are reached. (See Margenau and Watson, loc. cit. p.45). Hence at low pressures, Lorentz broadening would be expected to predominate.

If the foreign gas used to control the pressure consists of molecules with strong permanent polar fields, the action of these fields produces what is called Stark-effect broadening. Since, however, oxygen is not such a gas, we can ignore this mechanism.

According to Margenau and Watson (loc. cit. p.40) it is Lorentz broadening that is largely capable of explaining line-breadths in near infra-red spectra. This conclusion is derived from various experiments in the photographic region, and probably holds in the non-photographic, near infra-red. Of course, the Lorentz mechanism is not different in nature from the other "types" of molecular interaction--Resonance, Van der Waals, Stark-effect. It is merely a convenient way of describing one term in the complete expression for the total width of a line. It was first derived by Lorentz by considering that the process of absorption (or emission) is

interrupted at random intervals by collisions between molecules. He thereby introduced the concept of an "optical collision diameter", which for most gases is of the order of 10 A.U., and is larger than the kinetic-theory diameter obtained from viscosity or diffusion experiments.

The shape of a spectral line due to this mechanism is given by the Lorentz formula:

$$\mu = \frac{\frac{1}{\pi} S \alpha}{(\nu - \nu_0)^2 + \alpha^2} \qquad (1)$$

where S is the total intensity of the line defined by $\int_{-\infty}^{+\infty} \mu \, d\nu$, μ is the absorption coefficient at frequency ν, and α is the half-width of the line.

The half-width is given by:

$$\alpha = \frac{1}{\pi} (2\pi k T)^{1/2} n_1 \rho^2 \left(\frac{M+m}{Mm}\right)^{1/2} \qquad (2)$$

where ρ is the optical collision diameter, n_1 is the number of molecules per unit volume, M and m are the masses of the perturbing and absorbing molecule, respectively, k is Boltzmann's constant, and T is the absolute temperature.

It is readily seen that the half-width varies directly with the total pressure and inversely with the square-root of the temperature.

The applicability of collision broadening theory to H_2O band spectra in the infra-red has been discussed by Elsasser [2] who concludes "that collision broadening is practically the only cause of line width under atmospheric conditions". The reasoning could be applied to O_3 as well.

Matheson [3] has measured the increase of band absorption with thickness for the CO 4.66μ band, and concludes that the results are in agreement with the Lorentz shape.

A further question that cannot be overlooked is the effect of pressure on the total intensity of a spectral line, for unless we are sure of the constancy of line intensity, the dependence of transmission on pressure cannot be used to determine line widths.

The total intensity of a line, defined as $\int_{-\infty}^{+\infty} \mu d\nu$, depends on the transition probability and the equilibrium population of the molecular energy levels. The former depends on the form of the wave-function and hence, on the field of force; the latter depends on the energies of the levels and the temperature of the gas. In the case of collision broadening where the forces introduced by neighboring molecules merely affect the phase of a radiative transition, it is hardly probable that the wave-function is changed appreciably. Changes in the wave-functions serious enough to affect the transition probabilities would be expected at large densities, where considerable line asymmetry would also be introduced. Since the experiments were conducted at constant temperature, the population of the states was unaffected. Therefore, on theoretical grounds, the total intensity of the lines would be independent of pressure.

Unfortunately conclusive experimental work on the subject has not been done. G. Becker [4] examined the depen-

dence of line intensity on pressure in the HCL 3.5μ band and concluded that it is independent of pressure. His work is perhaps open to the objection that his resolution was not as complete as he thought. Further evidence of the constancy of line intensity can be found in the asymptotic approach to constant absorption at higher pressures, in the present work on ozone, and in the work of E. von Bahr [5] on N_2O_4, SO_2, NO_2, etc.

2. The Effect of Pressure on Band Absorption.

The qualitative hypothesis, that the increase of band absorption with increasing pressure is due to the broadening of the individual lines of the band, was first proposed by Chr. Fuchtbauer[6] in 1911. Ladenburg and Reiche[7] followed up this suggestion in 1913 with a mathematical analysis of the phenomenon.

To get a qualitative conception of the process, we consider a uniform band of lines at a low pressure so that the line-widths are much smaller than the separation, as in Fig. 1a. Allow the pressure to increase until the band looks like Fig. 1b. The maximum intensity decreases while the width increases so as to preserve the same total intensity, the area under each "line". That the absorption in case 1b. will be greater than in 1a is evident, because the re-distribution of the intensity has enabled the wings of the line to absorb more radiation than the reduced center will transmit. As the gas pressure increases, the lines start to overlap, Fig. 1c, and the total absorption continues to increase, but now more slowly because part of the line intensity acts in a spectral region already covered by a neighboring line. Finally, as in Fig. 1d, the lines have been greatly broadened by high pressure, and the overlapping is so complete that the composite intensity curve is flat. In this case, the absorption is at its highest, and higher pressure can merely slightly broaden the band as whole, and similarly, only slightly increase the absorption.

Recapitulating, the increasing pressure causes the

absorption (of a constant thickness, of course) to increase rapidly at first, then more slowly, and finally to level off.

This behavior was first observed and systematically studied by E. von Bahr, a student of K. Angstrom, during the years 1909 to 1912[5,8,9]. Fig. 2 is reproduced from her 1910 paper; it shows the increase in absorption with pressure for O_3, HCL, N_2O_4, SO_2, and NO_2. It may be remarked here that Fig. 2 contains the germ of the ultra-spectrometer method. The correlation between the steepness of approach to the maximum absorption and the moment of inertia of the absorbing molecule suggested the connection between the shape of the curve and the closeness of the lines in the band.

Similar studies of this pressure-effect were made by Hertz[10] in 1911 and Wimmer[11] in 1926. The former studied the CO_2 band at 14.7μ. The latter measured the absorption of the CO_2 4.3μ band under varying pressures of A, N_2, air, and H_2. The CO_2 results are similar to the results of E. von Bahr.

The phenomenon of band absorption can be discussed in terms of departures from Beer's law: (1) the absorption is dependent on total gas pressure, and (2) the absorption is not, in general, an exponential function of thickness. The dependence on gas pressure has been explained on the basis of pressure-broadening of the rotational lines. The departure from the exponential law is a result of the varying ab-

sorption coefficient in the band. Obviously, the dependence on thickness will be determined, at small thicknesses, mainly by the absorption coefficient at the central regions of the lines; at large thicknesses, by the wings of the lines; at intermediate thicknesses, by an "average" absorption coefficient. Effectively, then, the "absorption coefficient" varies with thickness.

A quantitative discussion of these departures from Beer's law will be found in Section 4.

3. The Measurement of Ozone Band Absorption.

In this section the experimental apparatus and procedure will be described.

The object was to measure the absorption of the ozone 9.6 μ band at varying ozone thickness* and under several different pressures. The necessary measurements were the total gas pressure, the thickness of ozone in the absorption cell, and the infra-red transmission at 9.6 μ.

The pressure was measured with an ordinary U-tube mercury manometer for pressures above 26 mm., and a 10 X McLeod gauge for lower pressures.

The thickness measurement was based on the absorption at 3110 A.U. and 3050 A.U. in the Hartley band of ozone, where the absorption coefficients have been experimentally investigated and Beer's law is obeyed.

The 9.6 μ absorption was measured simultaneously with an apophyllite reststrahlen receiver whose response curve centered nicely on the ozone band.

The total pressure was controlled by the addition of oxygen. According to experiments quoted by Margenau and

---

* The "thickness" of the absorbing gas is defined to be the path length of the gas layer reduced to 760 mm. pressure and 0°C.

and Watson (loc. cit. p.40), the effects of foreign gas pressures show no anomalous departures from Lorentz broadening in the infra-red. This was also found true in the CO_2 experiments, with N_2 and air, of Wimmer [11]. In addition, no significent difference was found in this research when, in two measurements, air instead of oxygen was added to the ozone.

The mixture of oxygen and ozone was produced by a silent-discharge ozonizer from Linde oxygen (99.5 O_2, 0.5 N_2) and was introduced into a 36-inch glass cell fitted with 3-inch optically worked NaCl windows, Fig. 3. The manometers were connected to the cell through a charcoal filter tube to protect the mercury against oxidation; a similar connection was provided for the pump. In the inlet line was inserted a liquid air condenser for freezing out the ozone from the approximately 5% mixture produced by the ozonizer, thus obtaining concentrations up to 40% in the cell.

The cell could rotate about a vertical axis to alternate between the ultra-violet path and the infra-red path. In addition, it was pivoted on a horizontal axis to alternate between the in-beam and out-of-beam positions, thus making possible control measurements of the source intensity. Flexible connections were made with Koroseal tubing [12] which resisted oxidation sufficiently to withstand several weeks of exposure, whereas ordinary rubber tubing would disintegrate in a few minutes. The use of stopcocks and the consequent

contamination by grease vapors was avoided by the use of pinch-clamps on the Koroseal connections.

The infra-red measurements were made with a reststrahlen receiver fitted with five apophyllite reflectors, the sensitive element of which was an evacuated thermocouple "blackened" with finely powdered crystalline quartz[13]. A KI plate served as a window to the thermocouple cell. The selectivity of apophyllite and the degree of elimination of scattered radiation is demonstrated by the fact that a clear glass plate interposed in a beam of sunlight reduced the response to 1/4% of the uninterrupted reading. Clear glass is opaque to the 9.66μ apophyllite reststrahlen but freely transmits the visible and near infra-red. The response curve of the instrument, measured with a grating spectrometer[13] and enclosed globar source, is shown in Fig. 4, superimposed on the ozone 9.6μ band, which was measured with the same spectrometer, similar thermocouple and similar source.

The source of infra-red radiation was a globar rod heated to about 1000° C, and enclosed in a water-cooled jacket to reduce temperature variations and blacken its emission. The intensity was held constant to less than 1% over a period of an hour by two parallel-connected iron-filament ballast tubes (type UV-876). The radiation was collimated by a 3-inch off-axis parabolic mirror.

A quartz-bulb tungsten lamp provided a continuous

source of ultra-violet radiation. A Hilger-Müller double quartz monochromator was used to isolate the proper wavelengths. The radiation emerging from the monochromator fell on a sodium photocell in a quartz bulb, the current then being amplified[14] and indicated by an L&N portable galvanometer. Two quartz lenses collimated and focussed the beam on the entrance slit. The current through the lamp was controlled by a Raytheon 250-watt transformer, resulting in a steady intensity that was constant to within 1% during a measurement, even during the busiest part of the day.

The determination of the ozone thickness is based on the Hartley band absorption where there is no pressure-effect and Beer's law applies. Two bands of about 6 A.U. width at 3050 and 3110 A.U. were selected, as shown in Fig.5, which is an intensity curve of the solar radiation passed by the atmospheric ozone. The two bands are also shown in Fig. 6, in comparison with the mercury spectrum. The upper spectrum illustrates the functioning of the monochromator: a number of bands at various wavelength settings are compared with the mercury spectrum.

The symbols used in the calculation of the thickness are:

μ_1, μ_2 - the absorption coefficients at 3050, 3110 A.U. respectively.

I_1, I_2 - the intensity transmitted by the ozone.

cell in the beam, at the two wavelengths.

I_1°, I_2° - the intensities with the ozone cell out of the beam.

X - the ozone thickness.

R - the ratio of I_2 to I_1

R_o - the ratio of I_2° to I_1°

I_{1c}, I_{2c} - the intensities transmitted by the empty cell.

t_{1c}, t_{2c} - the transmission of the rock-salt windows at the two wavelengths.

R_c - the ratio of t_{2c} to t_{1c}

The transmitted intensities are:

$$I_1 = I_{1c}\, 10^{-\mu_1 x} \quad ; \quad I_2 = I_{2c}\, 10^{-\mu_2 x} \tag{3}$$

Dividing, $$R = \frac{I_2}{I_1} = \frac{I_{2c}}{I_{1c}}\, 10^{(\mu_1 - \mu_2)x} \tag{4}$$

To correct for long term variations in source intensities, the cell was pushed out of the beam at each measurement of R.

$$R_o = \frac{I_2^\circ}{I_1^\circ} \tag{5}$$

$$I_{2c} = I_2^\circ t_{2c} \quad ; \quad I_{1c} = I_1^\circ t_{1c} \tag{6}$$

From (4), (5) and (6),

$$R = R_o R_c\, 10^{(\mu_1 - \mu_2)x} \tag{7}$$

Therefore, $$x = \frac{1}{\mu_1 - \mu_2} \log \frac{R}{R_o R_c} \tag{8}$$

The best value of $(\mu_{3050} - \mu_{3110})$ was taken as $1.50 \pm .10$ cm^{-1}. Of course, the thickness might have been

measured at one wavelength only, but a survey* of the various determinations of Hartley band coefficients showed that the absolute values differed greatly, but all the investigators were in close agreement on the relative values.

R_c was measured at various times during the research and was found to be quite constant at 0.977. R_o was measured as a control at each determination of the thickness: it was about 1.52. These measurements were accurate to about 1%, and although $(\mu_1 - \mu_2)$ is in doubt by as much as 10%, the relative thicknesses, and consequently all the conclusions of this study, are affected only by the lower figure.

The 9.6μ measurements were made in the following way. The transmission of the ozone and cell was determined from the ratio of the intensities with the cell alternately in and out of the beam. This was then corrected for the transmission of the empty cell, T_c (about 0.83), to obtain the transmission of the ozone itself, τ_π.

Because the ozone slowly decayed as the measurements progressed, the following regime was adopted. First the infra-red transmission was measured, rocking the cell in and out of the beam. Then the cell was rotated to the ultra-violet path, and R was measured with the cell in, then R_o with the cell out, and again R with the cell in. Finally the infra-red trans-

* The survey of the literature was made by Dr. K. Watanabe. He subsequently changed his "best value" to 1.40 on the basis of the work of Ny and Choong (15), but the calculations in this thesis are made with 1.50, the sole exception being Figs. 7,7a,8,9.

mission was again measured. Thus, the sequence was T, R, R_o, R, T. In calculating, the two T's were averaged, the two R's were averaged, and then $T._{av.}$, $R._{av.}$ and R_o were applied to the computation of the thickness and the infra-red absorption.

In this way, a series of measurements at different ozone thicknesses was made under the same total pressure. This was repeated at pressures of 722, 194, 104, 58, 25.8, 13.0, 6.0 mm. The thicknesses ranged up to about 5 mm. A typical page of data for one point is shown in Appendix B.

The results are shown in Fig. 7, where A_π, the infra-red absorption, is plotted against the square-root of the thickness, x, in cm. A cross-plot of the variation of absorption with pressure is shown in Fig. 8, at different thicknesses. The curves are compared with the straight lines representing $A \sim p^{1/4}$, in Fig. 9.

4. Theory of Band Absorption and Comparison With Experimental Results.

The calculation of band absorption has been treated by several authors: Ladenburg and Reiche [7] in 1913, Matheson [3] in 1932 and Elsasser [2,16] in 1938. The results of the calculation described herein are those of Elsasser.

Let us consider a band of uniformly spaced, equal lines, each having the Lorentz shape. If the spacing is d and the thickness of absorbing gas χ, then the absorption, defined as the fraction removed from the incident beam, is

$$A = \frac{1}{d}\int_{-\infty}^{+\infty}(1 - e^{-\mu x})\,d\nu \tag{9}$$

The absorption coefficient varies with frequency according to the equation:

$$\mu = \frac{\frac{1}{\pi} S\alpha}{(\nu-\nu_0)^2 + \alpha^2} \tag{10}$$

(See Sec. 1.)

For very small thicknesses, the absorption is proportional to thickness:

$$A = Sx \tag{11}$$

At pressures low enough so that the lines do not overlap appreciably, the following equation holds for large thicknesses:

$$A = \frac{2(S\alpha x)^{1/2}}{d} \tag{12}$$

Equation (12) is the asymptotic expansion of formula (9) at small $\frac{\alpha}{d}$ and large X. When X is in the moderate range used here, Elsasser has shown, (See Appendix D) that (12) should be replaced by the approximation,

$$A \approx 1.07 \frac{2(S\alpha x)^{1/2}}{d} + \text{an intercept} \qquad (13)$$

The square-root relation is due essentially to absorption in the wings of the lines, the core being practically opaque. Fig. 7 shows that the absorption at 6 mm. pressure is proportional to the square-root of the thickness. This may be regarded as direct support for the underlying hypothesis of Lorentz broadening, for the Lorentz shape is the only one that can produce this result.

At higher pressures this approximation fails, for when the half-width is comparable with the separation, the transmission is closely represented by:

$$T = e^{-\frac{Sx}{d}\tanh\frac{2\pi\alpha}{d}} \qquad (14)$$

This exponential relation holds more closely as $\tanh\frac{2\pi\alpha}{d}$ nears unity, that is, for values of $\frac{\alpha}{d}$ about .3 and larger.

In the case of the ozone band, $\frac{\alpha}{d}$ reaches .3 at about 100 mm. pressure (See Sec. 7 for the value of the line spacing). In this range, the absorption should be approximately an exponential function of thickness, approaching Beer's law, but the absorption coefficient depends on the pressure.

At still higher pressures, 722 mm. for example, the value of $\tanh\frac{2\pi\alpha}{d}$ is unity, and the formula becomes

$$T = e^{-\frac{Sx}{d}} \qquad (15)$$

This gradual approach to the exponential law as the pressure increases is verified by the curves of Fig. 7a, where the data of Fig. 7 are plotted on logarithmic scale. They also illustrate the asymptotic approach to a constant absorption coefficient. If we bear in mind that the analysis is based on an "ideal band" while the experimental data apply to a band composed of lines of irregular intensity and spacing, the agreement seems quite good.

To show how the absorption increases with pressure and levels off asymptotically, A was plotted against p for several thicknesses, in Fig. 8. These curves may be compared with those of E. von Bahr, Fig. 2. According to equations (2) and (12), the absorption at low pressures should increase with the square-root of the pressure. To test this, log A is plotted against log p, in Fig. 9. The slope over the range 6 mm. to 194 mm. is approximately 1/4.

Attention had been drawn to this fourth-root relation[17] as being in disagreement with the collision broadening explanation of the pressure-effect. The "anomaly" may, however, be exaggerated. The theoretical square-root relation is limited to low pressures, and indeed, the experimental points at the two lowest pressures show a slope of 1/3. Thus, the curves may be just emerging from the square-root region, the 6 mm. curve being the only one which is strictly a square-root curve in Fig. 7. Appendix E contains further remarks on the $P^{1/4}$ relation.

II. ULTRA-SPECTROMETER TECHNIQUE FOR INFRA-RED BANDS

5. The Ultra-Spectrometer Idea.

The basis of the ultra-spectrometer technique is a correlation between the shape of the pressure-effect curve and the closeness of the lines in the band.

If a constant thickness of absorbing gas is subjected to increasing pressure, the absorption increases, rapidly at first, then more slowly, and finally "saturating". This process has been described in Section 2. Saturation occurs when the lines have so broadened and overlapped that the composite absorption coefficient curve is quite level. Obviously, the closer the lines, the smaller the pressure required to attain saturation.

This relationship between "saturation pressure" and the density of lines in the band is obtainable from Fig. 2. If we list the bands in order of decreasing saturation pressure, they form the following sequence: HCL 3.4μ, NO_2 6.1μ, O_3 9.6μ, SO_2 7.4μ, N_2O_4 5.7μ. This is roughly the order of increasing molecular moment of inertia and probably increasing line density.

Used as a technique, the pressure-effect curve can yield information as to the line spacing in a new band. If the saturation pressure is low, the lines are close together; if it is high, they are wide apart.

Of course this qualitative method has its limitations. The most obvious is the absence of any very definite

criterion for determining the saturation pressure exactly. A further limitation is that the saturation pressure depends not only on the line spacing, but on such factors as the optical collision diameter and the mass of the molecule.

It was found possible to avoid these difficulties by applying the equations of Sections 1 and 4 to obtain a numerical value of the line spacing. This line spacing will be calculated at various wavelengths in the band. The pressure-effect curves obtained with a spectrometer will be used for this purpose. In the next section these measurements will be described.

6. Spectrometer Measurements of Ozone Band Absorption.

The object of this experiment was to measure the dependence of the ozone 9.6 μ absorption on total pressure and ozone thickness, as a function of wavelength.

The same cell and auxiliary equipment used in the previous experiment was used in this. The ozone thickness could not be directly measured, but had to be calculated on the basis of the reststrahlen results, Fig. 7, because both the Hilger monochromator and the reststrahlen receiver were in use at the time at Palomar Observatory for ozone height determinations.

The radiation form an enclosed globar rod heated to approximately 1000° C [18] was focussed by an aluminized spherical mirror on the center of the cell, and then focussed again by an opposite optical system* on the spectrometer slit.

A grating spectrometer fitted with a thermocouple receiver was used to measure the spectral intensity of the beam. The layout of the apparatus is shown in Fig. 10.

The spectrograph, described previously [13] had an F/3 optical system and an echellette grating**. The lines were ruled 19.63 μ apart over an area approximately five inches

* The symmetrical optical arrangement, Fig. 10, distorts the image less than the anti-symmetrical one. See reference (19).

**The grating was loaned by Prof. R. W. Wood to Dr. Strong, who permitted it to be used in this research.

square, with the flare at 14μ in a Littrow arrangement. The entrance and exit slits were each opened to a width corresponding to a spectral interval of .038μ at 9.6μ. By visual examination with white light, it was determined that the off-axis aberrations were smaller than the slit-width. Therefore, the resolution was probably about .06μ at 9.6μ, or a power of 160.

The radiation emerging from the exit slit was focussed by an elliptical mirror on a thermocouple of Bi-Sn and Bi-Sb wires coated with ThO_2 power and a thin lacquer binder. The thermocouple chamber was pumped by charcoal in liquid air: at "black vacuum" the sensitivity was 15 times that at atmospheric pressure. A rock-salt plate covered the aperture to the chamber. Rock-salt is non-selective at 9.6μ.

A reflector of sodalith was used in front of the entrance slit to isolate the 9.6μradiation from the much more intense short-wave radiation. To eliminate the small amount of short-wave radiation passed by the sodalith reflector (about 10% of the total), a Rubens shutter composed of a 1/10 mm. mica sheet and a compensating wire screen was used. The reflection curve of sodalith at 47° incidence and the transmission curve of mica at normal incidence are shown in Fig. 11, together with the ozone band and the radiation from a black body at about 1000° C.

Insulation of the spectrometer with aluminum foil was found sufficient to avoid appreciable drift of the galvan-

ometer: intensity measurements could be repeated to less than 1%. The voltage fluctuations of the line were reduced with a Raytheon stabilizing transformer. Constancy of the globar temperature was insured by draft protection of the surrounding water-cooled copper cylinder.

The procedure for taking absorption measurements was to fill the cell with a mixture of ozone and oxygen at a determined pressure, and record the absorption in steps of .07μ (1/2 mm. on the micrometer screw) across the band. The curves forward and backward were averaged to compensate for the gradual decay of ozone. Then the mixture was diluted at the same pressure, and the process repeated; and so on, until the ozone was almost gone. In this way, a series of absorption contours of different thicknesses at five different pressures, was obtained: 6.0, 13.0, 25.8, 50.0 and 722 mm. The results are shown in Figs. 12-16. A typical data page is described in Appendix B.

After each absorption contour was obtained, the corresponding thickness of ozone was computed in the following manner. Each contour was weighted with the response curve, Fig 4, of the reststrahlen receiver described above. The area under this weighted absorption curve represents the absorption that would be measured by the reststrahlen receiver.* With

---

* The necessity of numerically calculating the weighted absorption was ~~removed~~ avoided by the kind loan by Dr. W. Elsasser of his integrating machine capable of computing $\int^2 F(x)\,\Phi(x)\,dx$. $F(x)$ was the experimental absorption curve; $\Phi(x)$, the apophyllite response curve.

this "absorption", the ozone thickness could be read off the curves of Fig. 7.

Possible errors involved in this calculation were carefully investigated, and the combined probable error may be set at 2%. In addition, the method was checked for consistency by the following test: half the ozone was removed from a certain initial amount in the cell, and the calculated thickness before and after were found to be in the ratio of 2:1, allowing for a little decay. Thus, the relative thicknesses are quite accurate; hence, also the pressure-effect curves, and the relative line-densities. The uncertainty in the absolute line-densities is still governed by the uncertainty of the Hartley band coefficients, ± 5%.

The curves of Fig. 17 show the changes in the absorption contour of the same thickness of ozone at increasing pressures. The most significant effect of total pressure on band absorption can be demonstrated in terms of departures from Beer's law. Figures 18 - 23 illustrate the nature of the deviations.

The first three of these figures are logarithmic plots on which Beer's law would be a straight line. It is readily seen that the exponential law fits closest at 722 mm., where "saturation" has set in. The deviations become progressively larger at lower pressures.

The second three are square-root plots, testing the square-root relation (13). At 6 mm. pressure, while the

widths of the lines are still small compared with the separation, the curves are fairly straight. The deviations from straightness become more pronounced at higher pressures.

The curves of Figures 18 - 23 confirm rather well the calculations of Section 4. The low pressure data (6 mm.) are in accord with equation (13); the high pressure data (722 mm.) agree with equation (14).

7. The Density Contour of the Ozone 9.6 μ Band.

The agreement of the experimental results at 6 mm. pressure with the square-root equation, and the 722 mm. data with the exponential law, suggested the application of the band absorption formulas and the Lorentz line-width equation to the calculation of the "effective line spacing". We call it the "effective" spacing because the formulas are derived for bands of equally intense lines equally spaced. Such conditions do not exist in an actual band.

The equations to be used are the following:

From p. 6, $$\alpha = \frac{1}{\pi}(2\pi kT)^{\frac{1}{2}} n_1 \rho^2 \left(\frac{M+m}{Mm}\right)^{\frac{1}{2}} \qquad (16)$$

From p. 19, $$A = \frac{2\,(S\alpha x)^{1/2}}{d} \qquad (17)$$

From p. 20, $$T = e^{-\frac{Sx}{d}} \qquad (18)$$

From equation (16) the half-width of a spectral line can be calculated except for the uncertainty in the magnitude of the radiation cross-section. Since ρ is about 10 A.U., we may compute α to within a small numerical factor, c, probably between 1 and 5 for most gaseous molecules.

Applying equation (17) to the 6 mm. data in Fig. 21, we see that the slope of the straight lines is $2\,(S\alpha_6)^{\frac{1}{2}}/d$.

Therefore, $$(\text{slope}_6)^2 = 4\,\frac{S}{d} \times \frac{\alpha_6}{d} \qquad (19)$$

α_6 denotes the half-width at 6 mm. pressure. If we substitute the value of α_6 from equation (16), we obtain the

numerical value of $\frac{S}{d} \cdot \frac{c}{d}$.

The quantity S/d can be obtained by applying equation (18) to the slope of the logarithmic plots of the 722 mm. data, Fig. 18.

Then,

$$\text{Slope}_{722} = \frac{S}{d} \qquad (20)$$

Combining (19) and (20), we get a value of $\frac{d}{c}$ or d′, as we shall call it. d′ is the effective line spacing divided by a numerical factor between 1 and 5. We can introduce the term "line density" by dividing d′ into 10 cm^{-1}. (10 $cm.^{-1}$ is approximately the spectral width resolved by the spectrometer.) Fig. 24 shows the variation of this line density across the ozone 9.6μ band.

This density contour shows most spectacularly what has been achieved by this ultra-spectrometer technique: we are able to count the number of lines within a narrow, barely resolvable spectral interval, even when there are as many as two hundred lines in that interval!

8. The Structure of the Ozone Molecule.

Attempts to deduce the structure of the ozone molecule have been made by several investigators, the most recent being that of Hettner, Pohlman and Schumacher [20]. The troubles which beset all these investigators, other than that of manipulating ozone, can be reduced to two: the difficulty of purifying ozone from other gases, chiefly oxides of nitrogen, and the lack of the necessary resolving power to analyze the rotational structure.

We may remark here that the use of the present technique could have aided in solving both difficulties. First, by applying the technique to obtain curves like those of E. von Bahr, Fig. 2, the bands due to a heavy molecule like $N_2 O_5$ could have been distinguished from those of the O_3 molecule. The lower saturation pressure of the closely-spaced bands would have revealed $N_2 O_5$. And second, the lack of resolution could have been overcome by the determination of a density contour of the band, as described in Sec. 7.

The highest resolution ever applied to the analysis of the ozone spectrum was that of Gerhard [21], who investigated the structure of the 9.6 μ band with a spectrometer slit width of 0.3 cm^{-1}. (Ours is 6.3 cm^{-1}.) His spectrum is shown in Fig. 25. Gerhard decided that the ozone molecule is isosceles with an apex angle less than 60°. Such a molecule would exhibit the following fundamental vibrations:

ν_1 - a central-branch type,
ν_2 - a central-branch type, ν_2 probably $> \nu_1$.
ν_3 - a doublet type.

where, as usual, ν_1 is the "breathing" frequency, ν_2 is the "bending" frequency, and ν_3 is the unsymmetrical twisting frequency.

The long-wave half of the 9.6 μ band was called ν_3 because of its apparent doublet contour. The short-wave branch of the same band was called ν_2 because its contour could be taken for a central-branch type. ν_1 was supposed to correspond to the observed 7.4 μ band.

Gerhard's evidence was upset by the discovery of H.P.S. (loc. cit.) that the 7.4 μ band was due to N_2O_5, an impurity arising from the presence of nitrogen in the electrical discharge. These authors made a thorough survey of the infra-red spectrum of ozone from 1 μ to 27 μ with a prism spectrometer that could resolve 0.1 μ at 10 μ. Fig. 26 is reproduced from their paper.

In discussing the new evidence, H. P. S. dealt with all the possibilities:

The symmetric linear model was discarded because its selection rules would not permit the observed combination bands.

The unsymmetric linear model was discarded because the only possible perpendicular vibration, the 14 μ band, did not exhibit a null-branch. Also, Gerhard's spectra did did not indicate the required uniformly spaced lines.

The equilateral triangle was discarded because the observed bands could not be explained in terms of only one

active fundamental frequency.

The next simplest type was the isosceles triangle. Their calculations yielded the following possibilities:

(1) $\nu_1 = 9.65\mu$ (D), $\nu_2 = 14.1$ (D), $\nu_3 = 4.75$ (Z), $\alpha \geqslant 82°$

(2) $\nu_1 = 9.65\mu$ (Z), $\nu_2 = 13.8$ (Z), $\nu_3 = 14.4$ (D), $\alpha = 21.5°$

(3) $\nu_1 = 9.65\mu$ (D), $\nu_2 = 13.8$ (D), $\nu_3 = 14.4$ (Z), $\alpha = 32.5°$

(4) $\nu_1 = 9.65\mu$ (Z), $\nu_2 = 14.4$ (Z), $\nu_3 = 13.8$ (D), $\alpha = 25.3°$

(5) $\nu_1 = 9.65\mu$ (D), $\nu_2 = 14.4$ (D), $\nu_3 = 13.8$ (Z), $\alpha = 35.5°$

(6) $\nu_1 = 4.75\mu$ (Z), $\nu_2 = 9.65$ (Z), $\nu_3 = 14.1$ (D), $\alpha = 19.5°$

(The apex angle is 2α; D denotes doublet type, Z denotes central-branch type.)

(1) was declared improbable because of the unexpected large intensity of ν_1. (2), (3), (4) and (5) were declared improbable because they required the binding between closer atoms to be weaker than that between more separated atoms. This objection was also pointed out by Badger and Bonner [22].

H.P.S. concluded that (6) was the best possibility because:

(a) The relationship of the bond forces was reasonable.

(b) The ν_1 frequency, 4.75 μ, should be close to the frequency of the oxygen molecule, 6.3 μ.

(c) The 14.1 μ band is clearly a D-type band.

(d) Gerhard's spectrum of the 9.6 μ band might be interpreted to represent a Z-type band, but of this they are not too certain.

(e) The mean molecular heat, 300-476° K, is computed to be 9.8 cal., in fair agreement with 10.9 cal. measured by Lewis and Elbe.

The investigation here reported is not extensive enough to check the interpretations of all the bands. Had the experimental work been extended to other ozone bands, this check could have been obtained.

We can draw two conclusions, however, that decidedly strengthen the analysis made by H.P.S. The first is that the designation of the 9.6μ band as a Z-type band is in agreement with our line density contour, Fig. 24. The increase of almost 50% in density at the central maximum indicates an overlapping of the band by a central branch. Of course, the amount of this increase should not be taken too literally, it is modified by the ratio between the intensities of the overlapping branch and the other lines of the band.

The second conclusion is such as to support the rejection of the linear model. The line spacing in the branches on either side is approximately .06 cm^{-1}, on the basis of an estimated optical cross-section of 10 A.U. It is not to be expected, therefore, that the true line spacing in these side branches would be different from .06 cm^{-1} by more than a factor of 2. Now, the moment of inertia of a linear ozone molecule would probably be about 100×10^{-40} gm. cm^2. According to the formula, $\Delta\nu = h/4\pi^2 Ic$, this would result in a line spacing, outside the Q-branch, of 0.8 $cm.^{-1}$ It is exceedingly difficult to reconcile this with the approximate

measured value, .06 cm^{-1} .

But this close spacing is in agreement with the asymmetric rotator model, for each rotational level is split into (2j+1) levels, greatly increasing the number of transitions. True, it could also indicate an equilateral triangle configuration, but this was ruled out by other evidence, above.

9. Possible Applications and Limitations of the Method.

The ultra-spectrometer technique can be used in several ways to interpret molecular spectra:

Before examining an infra-red band in detail, the measurement of the variation of absorption with pressure can serve to distinguish a band due to a heavy molecule from the spectrum of a light one. Fig. 2 illustrates how bands of heavier molecules saturate at lower pressures than those of lighter molecules. Conversely, the magnitude of the saturation pressure can be of use in detecting impurity bands when the impurity is much heavier or lighter than the gas being studied.

The next most useful attack, is to compute an approximate value of the effective line spacing. This can be done by measuring the variation of the absorption with thickness in the square-root region (at a low pressure) and again in the exponential region (high pressure). Either a low power spectrometer or a reststrahlen receiver can be used for this purpose. If the value of the spacing turns out to be much smaller than that computed from $\Delta\nu = h/4\pi^2 Ic$, it can be concluded that the j-levels are not single but multiple. This would indicate a perpendicular band of a symmetrical-top molecule, or a band of an asymmetrical-top molecule. The band would probably not belong to a linear or spherical molecule, nor would it be the parallel band of a symmetrical top. Of course, allowance must be made for

possible large line densities in certain portions of the band even if the j-levels are single. For example, a central branch would introduce a large line density, or a band of a linear molecule with large vibration-rotation interaction might have a region of line convergence or parabolic return of the rotation lines. If the "effective" spacing is too large by a factor of two or three, the discrepancy may easily be due to fluctuating intensities in the rotational lines arising because of nuclear symmetries. In the limiting case, the effective spacing would equal the spacing between the lines of dominant intensity.

Further information about the band structure can then be deduced from a complete density contour of the band. As shown in this research, a central-branch band may be distinguished from a doublet type. The ultra-spectrometer method does not necessarily require as much work as was done in this thesis. Reduced to essentials:

1. Determine the appropriate region of pressure-saturation and the pressure region in which the square-root law obtains: the high and the low pressure regions.
2. Measure the variation of absorption with thickness at one high pressure and at one low pressure.
3. Calculate from the slopes of the two curves the ratio of half-width to spacing, and using the calculated Lorentz width, obtain the spacing.

The method obviously has certain limitations. For

instance, an unduly large (or small) collision diameter may be lead to a too large (or too small) value of the spacing. But this does not invalidate the comparison between line spacings in different parts of the band, or possibly, between bands of the same molecule.

The method is also affected by fluctuations in line intensities. Another weak spot is the uncertainty of applying the calculations to the wings of the band where intensities are sharply dropping off.

A more serious limitation is the possibility that other line-broadening agencies are present: for example, at high temperatures or at very low pressures the Doppler width becomes comparable with the Lorentz width, or, in the case of molecules with strong fields, Van der Waals or Stark-effect broadening may enter. But even these factors do not destroy the usefulness of the method. The qualitative conclusion, that those portions of the band in which the lines are more closely spaced will exhibit the more rapid pressure saturation, cannot be denied. If other types of broadening do enter, it is only the quantitative result that is uncertain. These other types of broadening can be detected, moreover, by the square-root test: at low pressures, it is the Lorentz shape which causes the absorption to be proportional to the square-root of thickness.

10. Further Problems.

Besides the application to the problem of the rotational line spacing of a band, the effect of pressure on band absorption is applicable to the problems of absolute intensities and of line shapes.

The subject of the intensities of lines and bands is one that has been considerably neglected. This is so, partly because of the greater difficulty of measuring intensities, and partly because the theory of transition probabilities has not been developed as vigorously as that of transition frequencies. However, it may be expected that both the theoretical and experimental study of spectral intensities will be stimulated when science turns to the problems of matter under extreme or unusual conditions.

For example, some aspects of electric arcs are attracting the attention of band spectroscopists: it is found, for instance, by means of the relative intensities of lines and bands, that the population distribution among the molecular states shows an anomalous departure from temperature equilibrium.[23] Of similar interest is the state of gases at high temperature and pressure that exists in the internal combustion engine. The development of high temperature by explosions and combustion of fuels is a field where spectroscopic studies of the transfer of energy into rotational and vibrational states are of interest. Perhaps the population of the states of a gas going through a shock-wave can be studied in

this manner. Applied physics is full of problems for the band spectroscopist interested in spectral intensities.

The present work is not directly applicable to all of these fields, but it does show how reliable intensity measurements may be made at ordinary conditions. The gas in question has merely to be subjected to increasing pressure by means of a neutral gas until the lines have broadened sufficiently for the pressure-effect to become negligible. Then, as shown in this paper, the absorption becomes exponential and the absorption coefficient may be integrated to obtain the total intensity of the band.

The subject of line shapes, especially in the infra-red, can also be treated by these methods. The question of what shape a line has, and what the broadening agency is, can be studied by measuring the dependence of band absorption on thickness and pressure. Matheson [3] has shown in this manner that the 4.7μ band of CO is composed of lines having the Lorentz shape. In this thesis, the agreement of the curves of Fig. 21 with the square-root law indicates a Lorentz shape for the O_3 9.6μ band.

Other types of molecules can be studied similarly. It would be of interest to see the deviations, if any, from Lorentz broadening in spectra of heavy molecules, molecules with peculiar symmetries, molecules with strong polar fields, etc. For instance, unpublished results of Dr. John Strong on the pressure-effect of the 11μ vibration of $C_2 H_6$,

which has been identified[24] as the bending frequence of the C - C bond, indicate either that the ethane lines haven't the Lorentz shape or that there is a background of very closely spaced lines as yet unrevealed by the spectrometer. However, more work has to be done on this. Another anomalous case is that of the HCN band at 1μ[25]. The line width has been found to increase with pressure more rapidly than the Lorentz theory, and is much greater with HCN pressure than an equivalent air pressure. It has not yet been explained.

Line shapes can be studied in still another way. We may call it a "Test for Similarity of Line Shapes." Consider a band of lines of possibly varying intensities but constant spacing. Assume the variation of line intensity across the band is slow enough that the lines within the slit width are of practically the same intensity. Then, if at a given pressure all the lines have the same shape except for the intensity factor (i.e., the same half-width, etc.), the variation of absorption with thickness at the different wavelengths will be similar. That is, if the curve at the center of the band is represented by $A_1 = f(x)$, the edge of the band will be represented by $A_2 = f(cx)$. Proof of this, and the application of the test to the ozone band are given in Appendix G. Obviously, the most fruitful application of this method is to the simpler gases, whose molecular bands have smooth intensity distributions and fairly constant spacings. For instance, the similarity of lines could be studied in CO, or CO_2, or the 10μ

bands of the methyl halides, etc.

In conclusion, we have shown the possibility of using the effect of pressure on band absorption as an ultra-spectrometer technique to aid in the analysis of infra-red spectra, greatly extending the usefulness of low power spectrometers. We have also shown how spectral intensities can be determined, and suggested applications to physical problems. Finally, band absorption experiments can be used to examine line shapes.

APPENDIX A - The Absence of Pressure-Effect in the Hartley Ozone Band in the Ultra-Violet.

The absence of pressure-effect was determined in the following manner, using the Hilger monochromator to measure the ultra-violet absorption.

The ozone thickness in terms of the ultra-violet absorption is given by,

$$\chi = \frac{1}{\mu_1 - \mu_2} \log \frac{R}{R_0 R_c}$$ (see p. 16)

The best values of R_o and R_c are:

$$R_o = 1.521 \pm .012$$

$$R_c = 1.026$$

Therefore, $R_o R_c = 1.560$

Measurements were started with the cell filled with a mixture of ozone and oxygen at 175 mm. pressure. A three-way stop-cock and a bulb of about 1 liter capacity were connected in the pump-line during this test.

R was first measured. Then the evacuated bulb was connected to the cell; the pressure dropped to 139 mm., part of the ozone and ozygen going into the bulb. Then the bulb was separated from the cell and evacuated while the new R was measured. This process was repeated successively ten times. Each time a constant fraction of the gas mixture was withdrawn.

Neglecting the slow decay of ozone, the fraction of the original pressure that remained after each withdrawal should have been the same as the fraction of ozone that remained.

The latter was measured by applying the above formula.

Constancy of the calculated fraction of ozone, using a constant value of $(\mu_1 - \mu_2)$, is then fairly conclusive proof of the absence of pressure-effect.

The data follow:

Withdrawal	Pressure	Measured $\left(\frac{R}{R_o R_c}\right)$	Log $\left(\frac{R}{R_o R_c}\right)$	Fraction Remaining
# 0	175.0	3.000	.4770	
1	139.0	2.305	.3626	.760
2	109.3	1.905	.2800	.772
3	86.0	1.650	.2174	.776
4	67.5	1.462	.1648	.759
5	53.0	1.346	.1288	.781
6	42.0	1.245	.0952	.739
7	32.5	1.181	.0722	.759
8	25.5	1.146	.0592	.820
9	20.5	1.106	.0438	.740

Average fraction of remaining ozone, $.767 \pm .020$

The fraction of the preceding pressure that remained after each withdrawal, averaged over seventeen measurements, is $.788 \pm .005$. The agreement is good, the ozone fraction tending to be lower than the pressure fraction because of some decay. We can conclude that pressure-effect in the Hartley band is absent.

APPENDIX B - Typical Data

1. A measurement of the infra-red absorption and the thickness of ozone, using the apophyllite reststrahlen receiver and the Hilger monochromator:

Time	UV: Off IR: Off	3050 In	Off Off	3110 Out			Calculations.
2:36	-.08	2.41	-.07	9.78	2.485	9.830	$T_\pi \times T_c =$
	-.03	2.43	-.04	9.79	2.465	9.815	$\frac{2.481}{9.815} = .2528$
1-R	-.01	2.48	-.01	9.80	2.490	9.800	
	+.01	2.49	00		2.485		
2:49	-.17	2.33	-.22	8.08	2.525	8.275	$R =$
	-.17	2.38	-.18	8.07	2.555	8.240	$\frac{8.268}{2.546} = 3.248$
U-V	-.16	2.38	-.19	8.13	2.555	8.290	
	-.13	2.39	-.19		2.550		
3:06	+.06	6.53	.07	9.90	6.465	9.825	$R_o =$
	+.08	6.49	.07	9.84	6.415	9.745	$\frac{9.797}{6.414} = 1.528$
U-V	+.12	6.47	.09	9.91	6.365	9.815	
	+.10	6.50	.08		6.410		
3:22	.00	2.57	-.02	8.33	2.580	8.335	$R =$
	+.01	2.58	-.02	8.37	2.585	8.365	$\frac{8.363}{2.581} = 3.240$
U-V	+.03	2.58	-.03	8.39	2.580	8.390	
	+.03	2.58	-.03		2.580		
3:40	-.08	2.43	-.09	9.70	2.515	9.785	$T_\pi \times T_c =$
	-.08	2.44	-.08	9.70	2.520	9.780	$\frac{2.518}{9.783} = .2572$
I-R	-.08	2.44	-.08		2.520		

3:50 Pressure: 819 + 88 - 184 = 723 mm.
Temperature: 83° F.

Avg. value, $T_\pi \times T_c = 1/2\ (.2528 + .2572) = .2550$
Avg. value, $R/R_oR_c = 1/2\ (3.248 + 3.240)\ /1.528 \times 1.026 = 2.070$
I - R Absorption, $A_\pi = 1 - .2550/.837 = .695$
Ozone Thickness, $x = \log 2.070/1.50 = .211$ cm.

2. A measurement of the absorption contour, using the infra-red spectrometer, and a calculation of the corresponding ozone thickness:

Position, Wavelength Screw	Galvanometer Rdgs. Mica	Screen	Mica	Net Deflection	Standard Deflections Cell Out	Corrected Absorption
12.	11.74	20.69	11.82	8.91	10.65	6.1
13.	11.88	22.38	12.07	10.40	13.71	14.9
14.	12.27	20.81	12.28	8.53	15.38	37.8
14.5	12.25	23.43	12.33	11.14	15.70	20.4
15.	12.37	21.44	12.41	9.05	15.86	36.0
16.	12.49	22.82	12.60	10.27	16.07	28.2
17.	12.74	23.72	12.86	10.92	15.39	20.4
18.	13.15	25.35	13.30	12.12	15.10	9.9
19.	13.60	25.06	13.82	11.35	13.13	3.0
19.5	13.92	24.47	14.02	10.50	11.95	1.3
18.5	13.82	25.77	13.98	11.87	14.18	6.1
17.5	13.47	25.12	13.42	11.67	15.37	14.8
16.5	13.08	23.60	12.99	10.56	15.67	24.4
16.	12.84	23.07	12.78	10.26	16.07	28.3
15.5	12.60	22.73	12.54	10.16	16.11	29.2
14.5	12.32	23.48	12.32	11.16	15.70	20.1
13.5	12.17	20.84	12.15	8.68	14.91	34.6
13.	12.04	22.42	12.06	10.37	13.71	15.1
12.5	11.96	22.07	11.91	10.13	12.03	5.5
12.	11.78	20.72	11.72	8.97	10.65	5.4

Source intensity, measured three times during measurements, at wavelength 15.0 : 16.65, 16.65, 16.63 ; avg., 16.64

Standard intensity at 15.0 : 15.86

Intensity correction factor: $\frac{15.86}{16.64} = .952$ Empty cell Transmission, .850

Pressure: 25.85 mm.

Temperature: 25.9° C

Total Absorption, weighted by reststrahlen response curve, 1365 area units.

Area under reststrahlen response curve, 4840 units.

Calculated reststrahlen absorption $= \frac{1365}{4840} = 28.2 = A_\pi$

From Fig. 7, $\sqrt{x} = 1.008$

$\therefore$ Ozone thickness, $x = 1.016$ mm.

APPENDIX C -- Calculation of Line Density Contour

Following the method of calculation outlined in Section 7:

$$\frac{\alpha_6}{d} = 1/4 \ \frac{(\text{slope}_6)^2}{(\text{slope}_{722})} \qquad (21)$$

Further, the half-width can be expressed as follows:

$$\alpha = \frac{1}{\pi} \rho^2 n_1 (2\pi k T)^{1/2} \left(\frac{M+m}{mM}\right)^{1/2} \frac{1}{U} \quad \text{cm.}^{-1} \qquad (22)$$

The following numerical values can be substituted:

$m_{O_3} = 48 \times 1.65 \times 10^{-24}$ gm.

$M_{O_2} = 32 \times 1.65 \times 10^{-24}$ gm.

$T = 296^{\circ}$ K.

$k = 1.37 \times 10^{-16}$ ergs $-C^{\circ}{}^{-1}$

$\rho = \sqrt{c} \times 10$ A.U. ; $\rho^2 = c \times 10^{-14}$ cm^2

$n_1 = \frac{P}{T k} = 3.28 \times 10^{17} \times h_{\text{cm. mercury}}$

$v = 3 \times 10^{10}$ cm. -sec^{-1}

Therefore, $\alpha = .00164 \times c \times h_{\text{cm.}}$ cm^{-1} (23)

and, $\alpha_c = .000984\, c$

Defining $d' = d/c$, the effective spacing is given by

$$d' = .0039 \ \frac{(\text{slope}_{722})}{(\text{slope}_6)^2} \qquad (24)$$

From Figs. 18 and 21, we get the values of the slopes tabulated below, and we can then compute d' at each wavelength.

Wavelength Setting	Slope 722	Slope 6	Calculated d′	Effective Line Density 10/d′
13.0	.200	.116	.056	179
13.5	.780	.215	.064	156
14.0	.919	.225	.069	145
14.5	.298	.146	.053	189
15.0	.686	.240	.045	222
15.5	.667	.197	.065	154
16.0	.667	.194	.067	149
16.5	.510	.169	.068	147
17.0	.345	.143	.064	156
17.5	.210	.116	.059	169
18.0	.125	.082	.071	141

The variation of 10/d′ with wavelength is plotted in Fig. 24.

APPENDIX D -- The Value of the Intercept in the Square-root Relation*.

From the calculations of Ladenburg and Reiche [7], we can get the following expression for the fractional absorption of an "ideal band" of uniformly spaced, non-overlapping lines:

$$A = 2\pi \frac{\alpha}{d} m e^{-m} \left\{ J_0(im) - i J_1(im) \right\} \quad (25)$$

where α = half-width, d = line spacing, and m is the dimensionless quantity, $\frac{S x}{2\pi\alpha}$. S is the total intensity of a line, and x is the path thickness.

In the region of small m, the absorption follows a linear law:

$$A \longrightarrow \frac{S}{d} x \quad (26)$$

In the region of large m, the absorption approaches asymptotically a square-root relation:

$$A \longrightarrow 2 \frac{(S \alpha x)^{\frac{1}{2}}}{d.} \quad (27)$$

Elsasser plotted the function $m e^{-m} \left\{ J_0(im) - i J_1(im) \right\}$ against $m^{\frac{1}{2}}$ and found:

(a) - A parabolic region, $0 < \sqrt{m} < .5$

(b) - A long, almost linear region, $.5 < \sqrt{m} < 3$

(c) - A region of approach to the asymptote, $f(m) = \sqrt{\frac{2m}{\pi}}$
$3 < \sqrt{m} < \infty$

The pseudo-linear region, he found, can be represented by $F(m) = a\sqrt{m} - c$. a is approximately .86, whereas the slope of the asymptote is $\sqrt{\frac{2}{\pi}}$ or .80.

But the intercept, at $A = 0$, is

$$(\sqrt{m})_0 = 0.21 \quad (28)$$

* This evaluation of the intercept is due to Dr. W. Elsasser.

This leads to:

$$\frac{S}{\alpha} = \frac{.28}{X_o} \quad , \tag{29}$$

where X_o is the thickness intercept on the square-root plot, Fig. 21.

We can thus get an experimental value of S/α to compare with the value obtained from the slopes. It is more instructive to compute a new value of d' instead, and compare it with the previous values.

From Appendix C,

$$d' = .00095 \frac{d}{\alpha_c} = .00095 \frac{S/\alpha_c}{S/d} \tag{30}$$

Substituting for S/α_c:

$$d' = \frac{.00027}{X_o (\text{slope}_{722})} \tag{31}$$

The following table shows the intercepts, the calculation of d', and a comparison with the previous d':

Wavelength Setting	Slope_{722}	$X_o^{\frac{1}{2}}$	d'	d' from Appendix C
13.0	.200	.15	.068	.056
13.5	.780	.00	∞	.064
14.0	.919	.00	∞	.069
14.5	.298	.13	.054	.053
15.0	.686	.08	.062	.045
15.5	.667	.09	.050	.065
16.0	.667	.09	.050	.067
16.5	.510	.10	.053	.068
17.0	.345	.11	.065	.064
17.5	.210	.15	.057	.059
18.0	.125	.20	.054	.071

The values of d' calculated from the intercepts are in fair agreement with the values computed from the slopes, except that the accuracy of the intercepts is not

good enough to warrant a line-density contour. The approximate agreement, however, greatly strengthens the theory.

APPENDIX E - On the $P^{\frac{1}{4}}$ Formula for Band Absorption.

Research in the distribution of radiative heat transfer in the atmosphere has stimulated interest in the dependence of band absorption on pressure. Calculations based on the ozone measurements [26] and on the measurements of G. Hertz on CO_2 [10,17] indicate that the absorption, over a wide range, is closely proportional to the fourth-root of the pressure.

Strong and Watanabe [17] thought that this might be evidence that line-broadening is proportional to the square-root of the pressure, in disagreement with the Lorentz theory.

In this section it will be shown that the $P^{\frac{1}{4}}$ relation is consistent with Lorentz theory. We will use the results of Appendix C to make a numerical calculation of the dependence of absorption on pressure.

In Section 4, it is shown that at low pressures,

$$A = \frac{2\,(S \alpha x)^{\frac{1}{2}}}{d} \qquad (32)$$

Extending over a somewhat longer range, the following formula also holds at low pressures [16]:

$$T = 1 - \phi\left[\frac{(\pi S \alpha x)^{\frac{1}{2}}}{d}\right] \qquad (33)$$

where ϕ is the probability integral.

At high pressures, the exponential law sets in:

$$T = e^{-\frac{S}{d} x \tanh \frac{2\pi\alpha}{d}} \qquad (34)$$

To plot these equations numerically, take $x = 1$ mm. of ozone, and the ultra-spectrometer results:

$$\frac{\pi\alpha}{d} \sim .01\, p_{mm} \; ; \; \frac{S}{d} \sim 0.8$$

These are "average" values for the whole band. The three curves (32), (33), and (34) plotted between 5 mm. and 500 mm. pressure are shown in Fig. 27.

Since the square-root and the ϕ curves are expected to hold at low pressures, and the exponential at high pressures, the dotted curve is faired in to represent the transition. If now the dotted curve is re-plotted on a log-log scale similar to Fig. 9, we see that is very similar to the curves of Fig. 9 and has an average slope of 1/4.

Thus, the fourth-root is not due to failure of Lorentz theory, and the conclusion that the line-width is proportional to the 1/2-power of the pressure is not valid. The mistake consisted in applying to this pressure-range the square-root equation.

Also, it appears that we are justified in applying the square-root equation to the 6 mm. data of ozone: 6 mm. seems to be just on the verge of the $P^{\frac{1}{2}}$ region.

APPENDIX F - A Second Method of Calculating Density Contours.

An alternative method for calculating the line density is based on the shape of the approach to saturation. Qualitatively, the closer the lines, the sharper will be the approach; the farther apart the lines, the more gradual the approach.

For numerical calculation, we can use equation (14),

$$T = e^{-\frac{Sx}{d} \tanh \frac{2\pi\alpha}{d}}$$

If we take logarithms twice,

$$\log (-\log T) = \text{const} + \log \tanh \left(\frac{2\pi\alpha}{d}\right) \quad (35)$$

From equation (23),

$$\frac{2\pi\alpha}{d} = .0010 \frac{h}{d'} \quad (36)$$

where h is the pressure in mm. of mercury, and d' is the effective line spacing in cm^{-1}.

Substituting in (35),

$$\log (-\log T) = \text{const}\ (x) + \log \tanh (.0010 \frac{h}{d'}) \quad (37)$$

This equation is then applied to the experimental values of T and h (at constant thickness, x) to obtain d'.

If d' were known, a graph of the left member against the right member would have a slope of 45° in the saturation region. The method, then, is to plot equation (37) for various assumed values of d', and that value of d' which gives the curve a 45° slope at the upper end is the true value. Obviously, this region will not be a long one because log (- log T) is exactly constant when saturation is reached. Therefore, the

curve should be expected to make just a short asymptotic approach to the 45° slope.

Fig. 28 shows such a set of curves. From these it appears that $d' \sim .075$ cm.$^{-1}$ at wavelength 15.0

A simpler application of the same idea is the following: Take two pressures which are in this region of saturation. In this case, we take 58 mm. and 722 mm. At each of these pressures, measure the absorption contour of the same thickness of ozone (1.11 mm. was selected.) At each wavelength, calculate log (-log T) for each pressure, and get the difference, Δ log (-log T). Similarly compute Δ log tanh$(.0010\, h/d')$ ~~(.0010 h/d)~~ as a function of d'. Then, if both the 58 mm. absorption and the 722 mm. absorption are in the exponential region,

$$\Delta \log \tanh (.0010\ h/d') = \Delta \log (-\log T) \qquad (38)$$

From this equation the correct value of d' can be determined at each wavelength.

Fig. 29 is a density curve obtained in this way. The agreement with Fig. 24 is quite good. The numerical values are slightly different, but the contour has a similar shape.

APPENDIX G - Test for Similarity of Line Shapes

Two spectral lines are said to be "similar" in shape if their distributions with respect to wavelength are identical, although the intensities may be different. In the case of a Lorentz shape, similarity would require equal widths.

Since the absorption is expressed by,

$$A = \int (1 - e^{-\mu(\nu)x})\, d\nu \qquad (39)$$

the curves of absorption against thickness should be reducible to a common curve by suitable expansion or contraction of the X-axis.

Conversely, the test for similarity is to see whether the curves can be reduced by change of scale.

Note that this test will fail at high pressures, because the transmission curves will all be exponential regardless of the individual line shapes. In the case of Lorentz broadening, it will also fail at low pressures, because the absorption will be proportional to the square-root of the thickness whether the widths are equal or not. At an intermediate pressure, however, where the lines just partially overlap, the shape of the absorption-thickness curve will be dependent on the line shape. For the same reason, the method tests not only similarity of line shapes, but also equality of the ratio of width to spacing, and the similarity of intensity fluctuations.

In the following table, four regions of the band are compared at 58 mm. pressure (Fig. 22). The 16 mm. curve is taken as the standard curve. Thicknesses corresponding to the same absorption at wavelengths 14, 15, 17 are compared with the thickness at wavelength 16.

Ratio of $\frac{X_{\lambda}}{X_{16}}$

Absorption	X_{14}/X_{16}	X_{15}/X_{16}	X_{16}/X_{16}	X_{17}/X_{16}
.20	.59	.79	1.00	1.93
.30	.58	.72	1.00	1.82
.40	.58	.72	1.00	1.82
.50	.55	.69	1.00	1.88
.60	.58	.67	1.00	—
.70	.58	.64	1.00	—

It is seen that the 14, 16, 17 mm. curves are closely similar in shape, whereas the 15 mm. curve is different from these. This also agrees with the results shown in Fig. 24: the spacing at 15 mm. is smaller than at either 14, 16, or 17 mm. Because the spacing is known to be different, we can draw no conclusion about the line shapes.

SYMBOLS AND NOTATION

μ - Absorption coefficient.

S - Total intensity of a line.

ν - Spectral Frequency.

α - Lorentz half-width of a line.

k - Boltzmann's constant.

T - Absolute temperature.

n_1 - Number of molecules per unit volume.

ρ - Optical collision diameter.

M - Molecular mass of neutral gas.

m - Molecular mass of absorbing gas.

I - Transmitted intensity.

t - Transmission of rock-salt windows.

R - Ratio of intensities at wavelengths 3050 and 3110 A.U.

x - Thickness of ozone.

T_π - Transmission of the ozone band.

A_π - Absorption of the ozone band.

p - Total gas pressure in cell.

d - Spacing between the lines of a band.

A - Absorption of an "ideal" band.

T - Transmission of an "ideal" band.

α_6 - Lorentz half-width at 6 mm. pressure.

c - Numerical factor describing uncertainty in ρ

d' - Effective spacing between lines.

ν_1 , ν_2 , ν_3 , - The three fundamental frequencies of a triangu-

h - Planck's constant. /lar molecule.

I - Greatest moment of inertia of molecule.

c - Velocity of light.

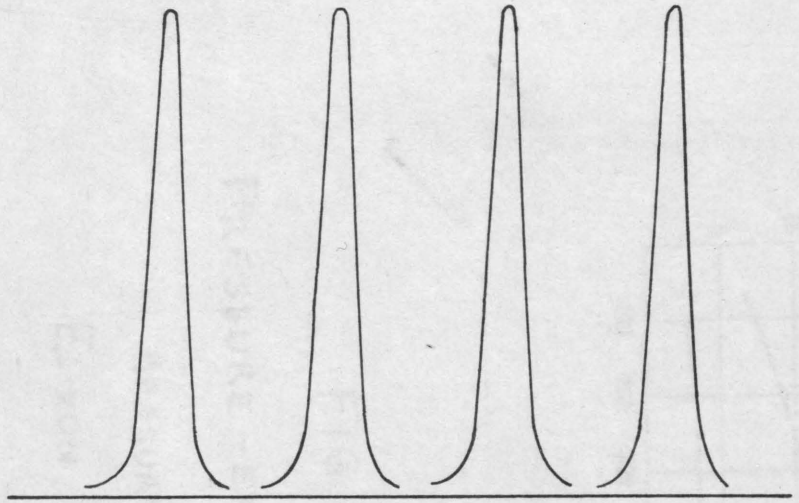

FIG. 1a

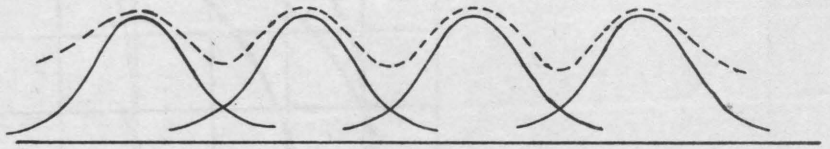

FIG. 1c

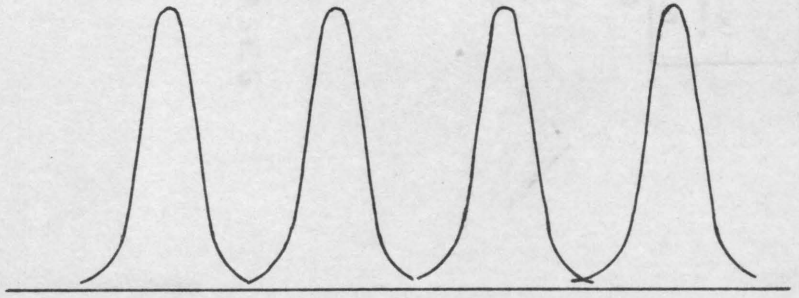

FIG. 1b

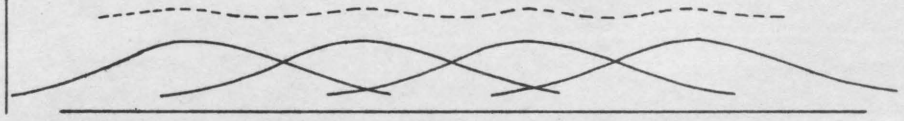

FIG. 1d

PRESSURE BROADENING OF LINES IN A BAND

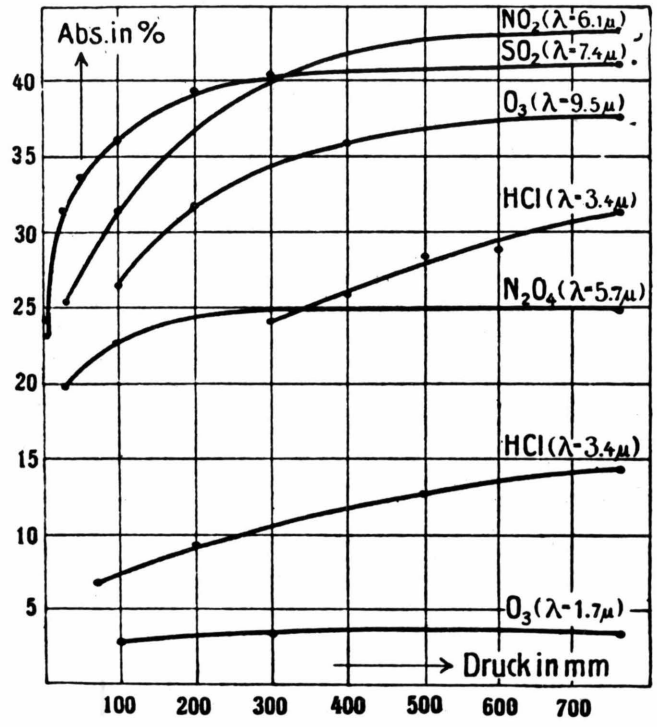

FIG. 2

PRESSURE-EFFECT IN GASES

MEASURED BY

E. VON BAHR

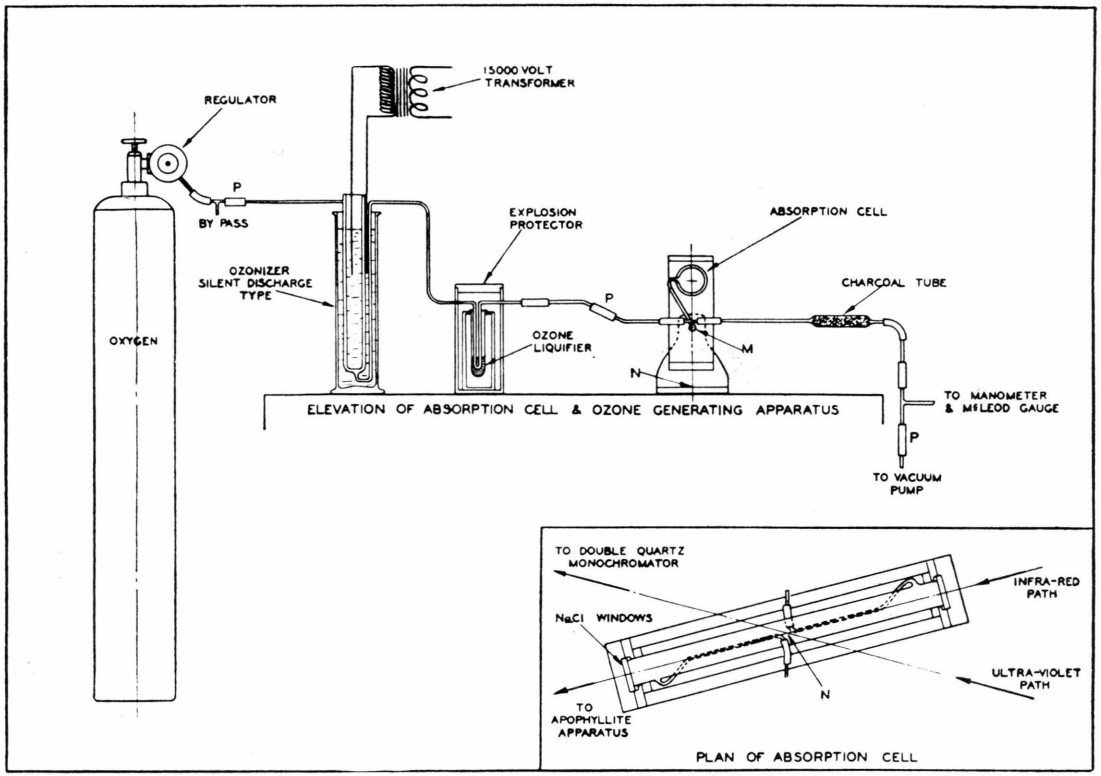

FIG. 3 – APPARATUS FOR OZONE MEASUREMENTS

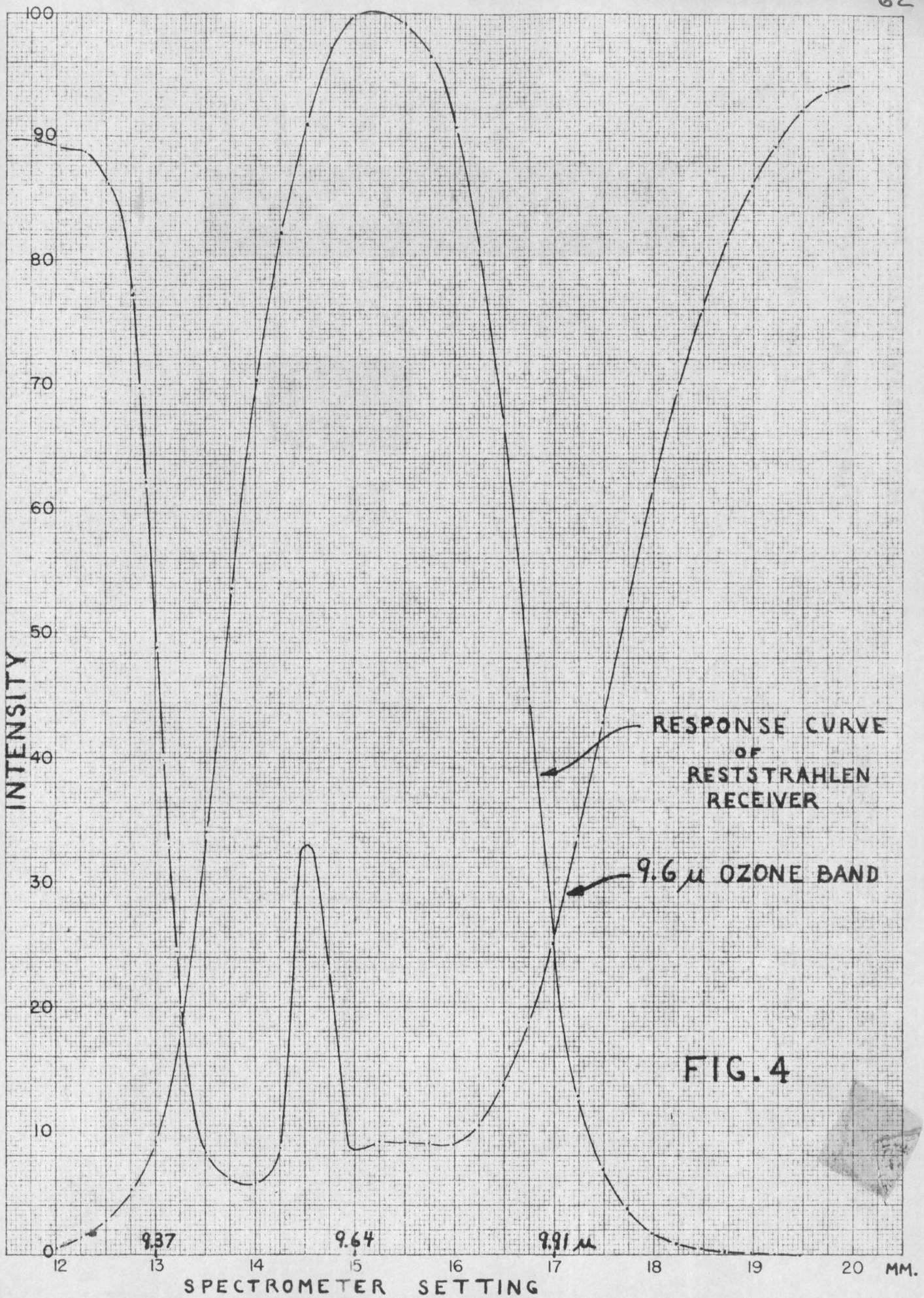
100
90
80
70
60
50
40
30
20
10
0
INTENSITY
RESPONSE CURVE OF RESTSTRAHLEN RECEIVER
9.6 μ OZONE BAND
9.37
9.64
9.91 μ
12
13
14
15
16
17
18
19
20
MM.
SPECTROMETER SETTING

FIG. 4

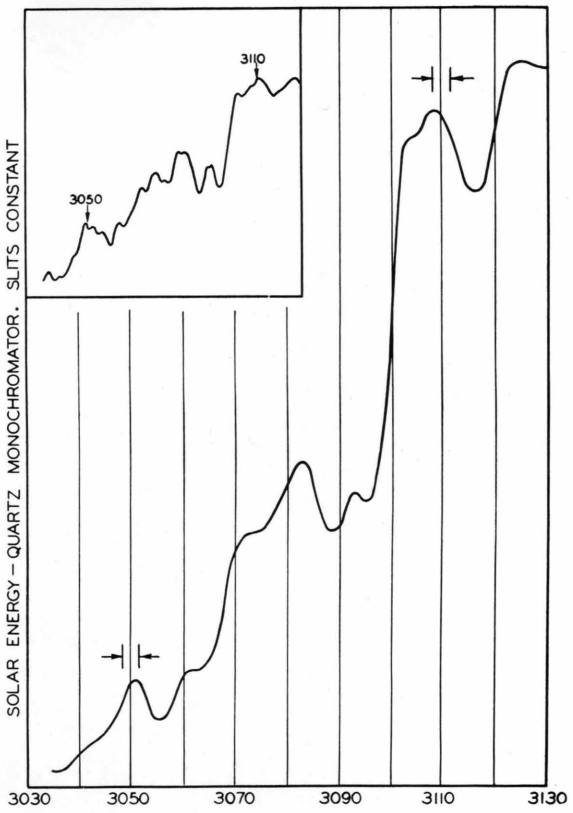

FIG. 5

THE HARTLEY BAND OF OZONE

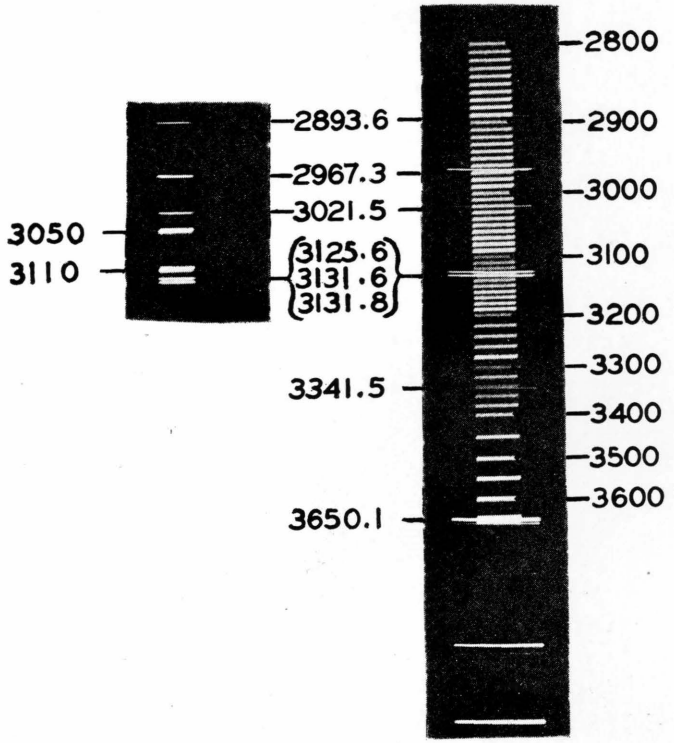

FIG. 6

SPECTROGRAM SHOWING THE TWO ULTRAVIOLET WAVELENGTHS.

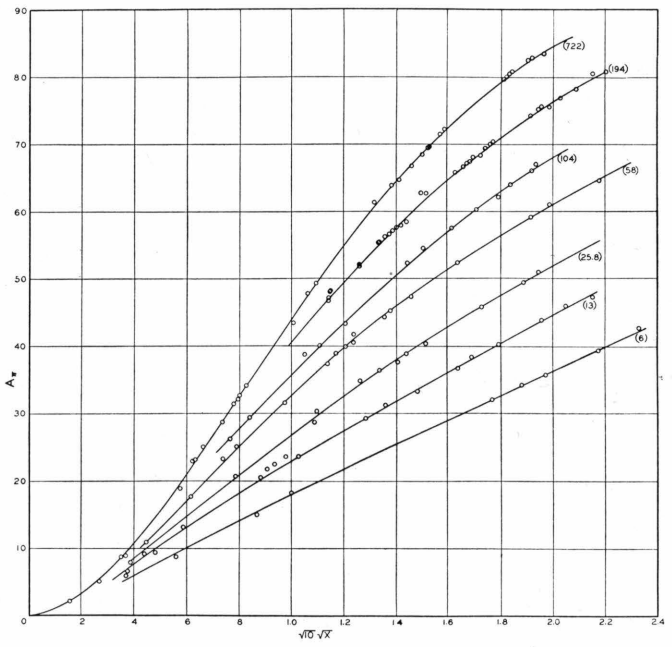

FIG. 7 – OZONE BAND ABSORPTION VS. THICKNESS$^{1/2}$, AT SEVEN PRESSURES.

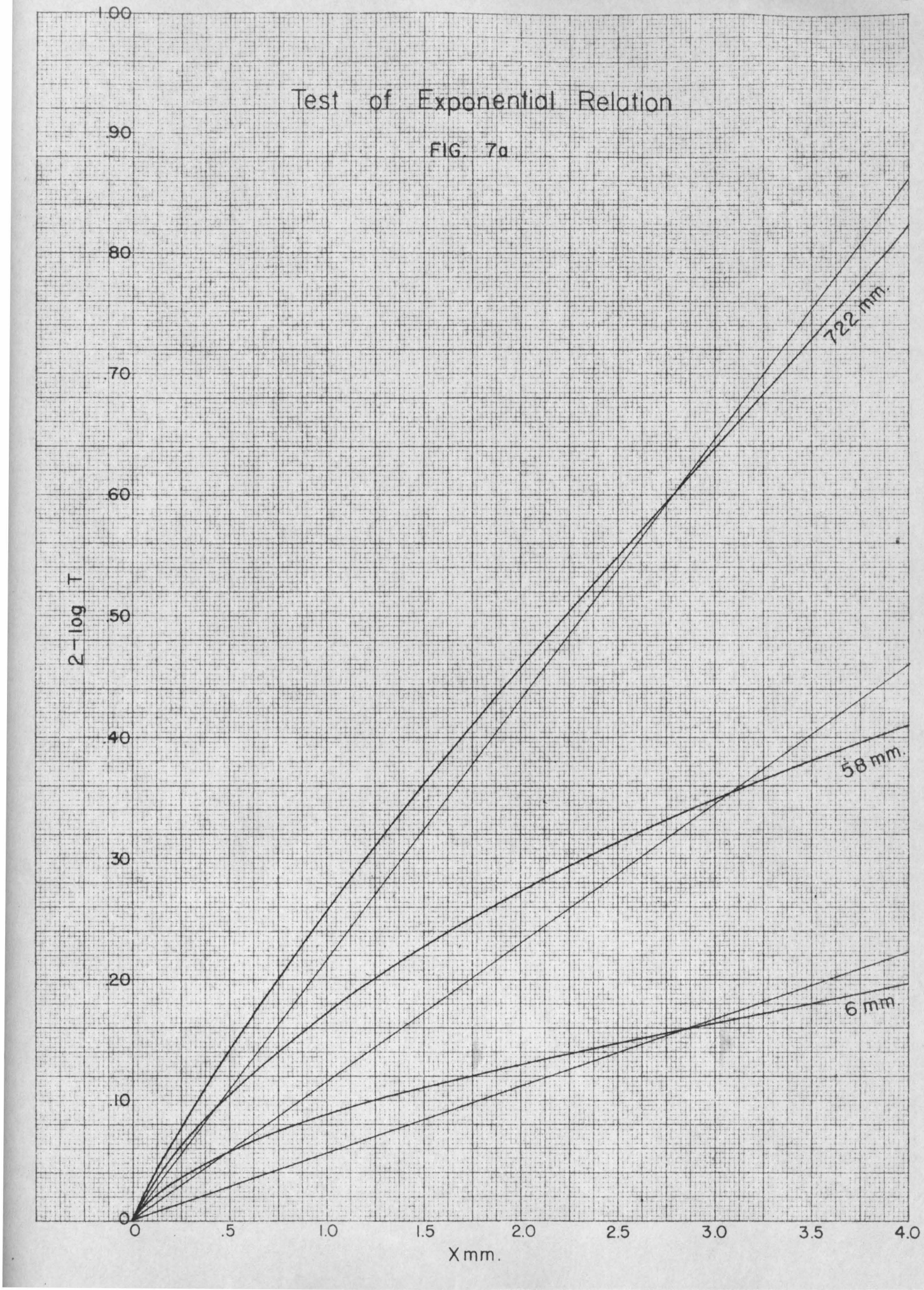
Test of Exponential Relation
FIG. 7a
1.00
.90
.80
.70
.60
.50
.40
.30
.20
.10
0
2 − log T
722 mm.
58 mm.
6 mm.
0
.5
1.0
1.5
2.0
2.5
3.0
3.5
4.0
X mm.

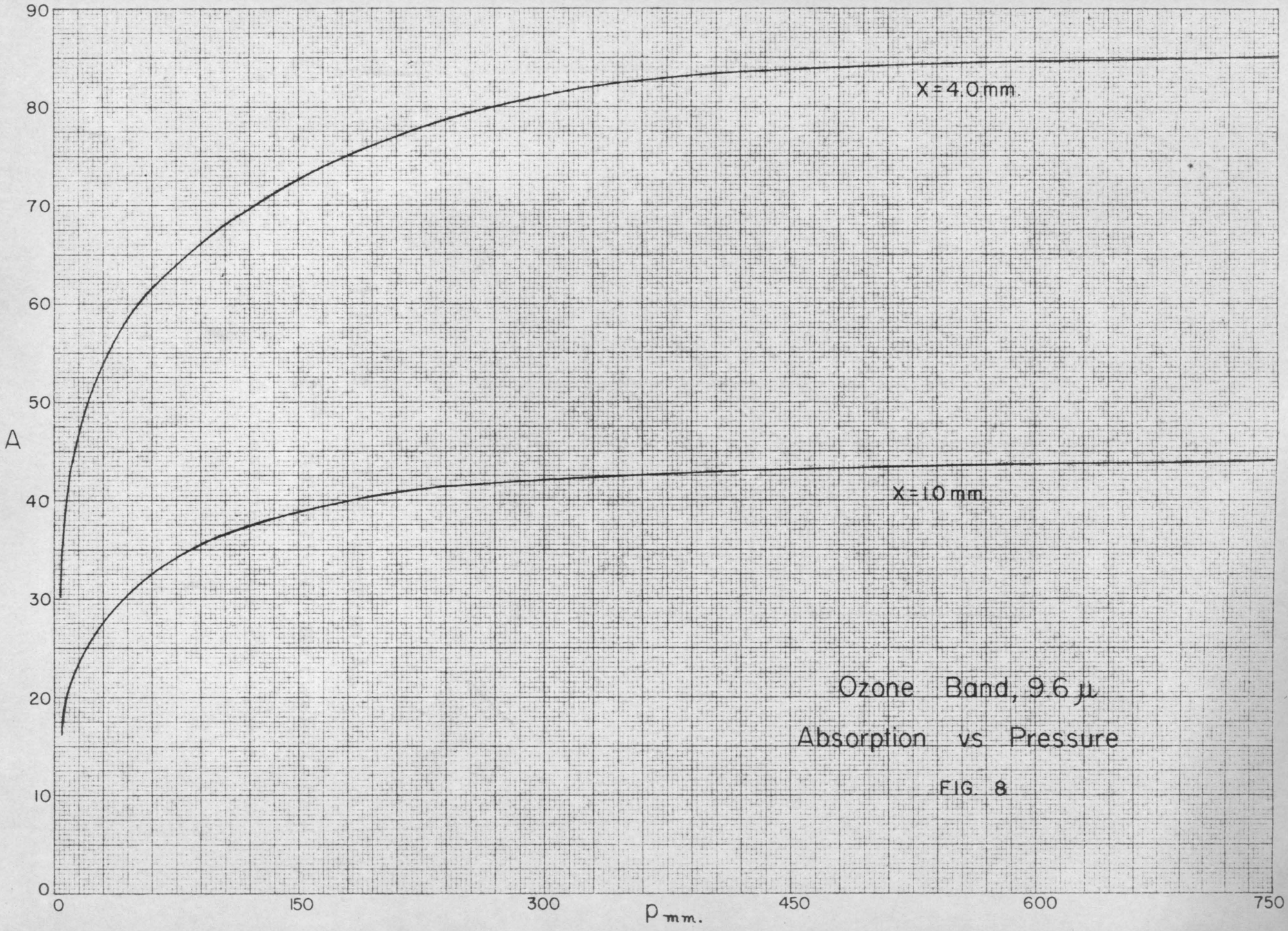

Ozone Band, 9.6 μ

Absorption vs Pressure

FIG. 8

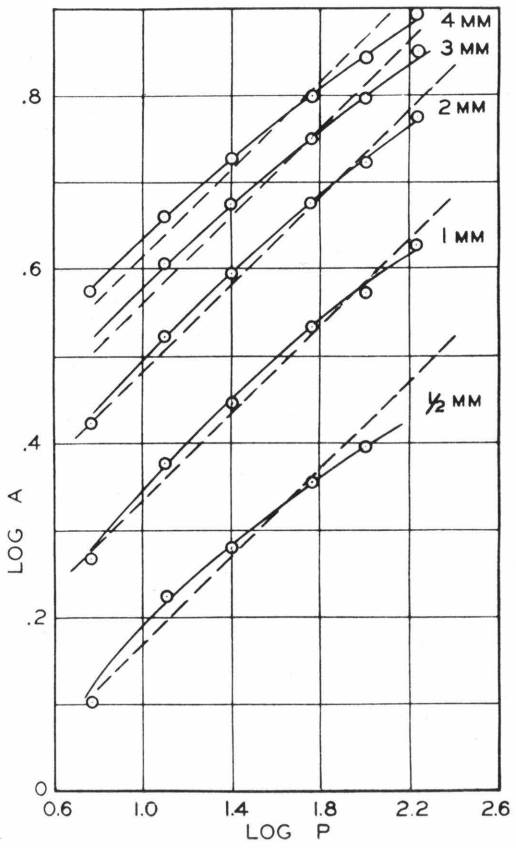

FIG. 9 — THE EMPIRICAL $P^{1/4}$ - RELATION BETWEEN ABSORPTION AND PRESSURE

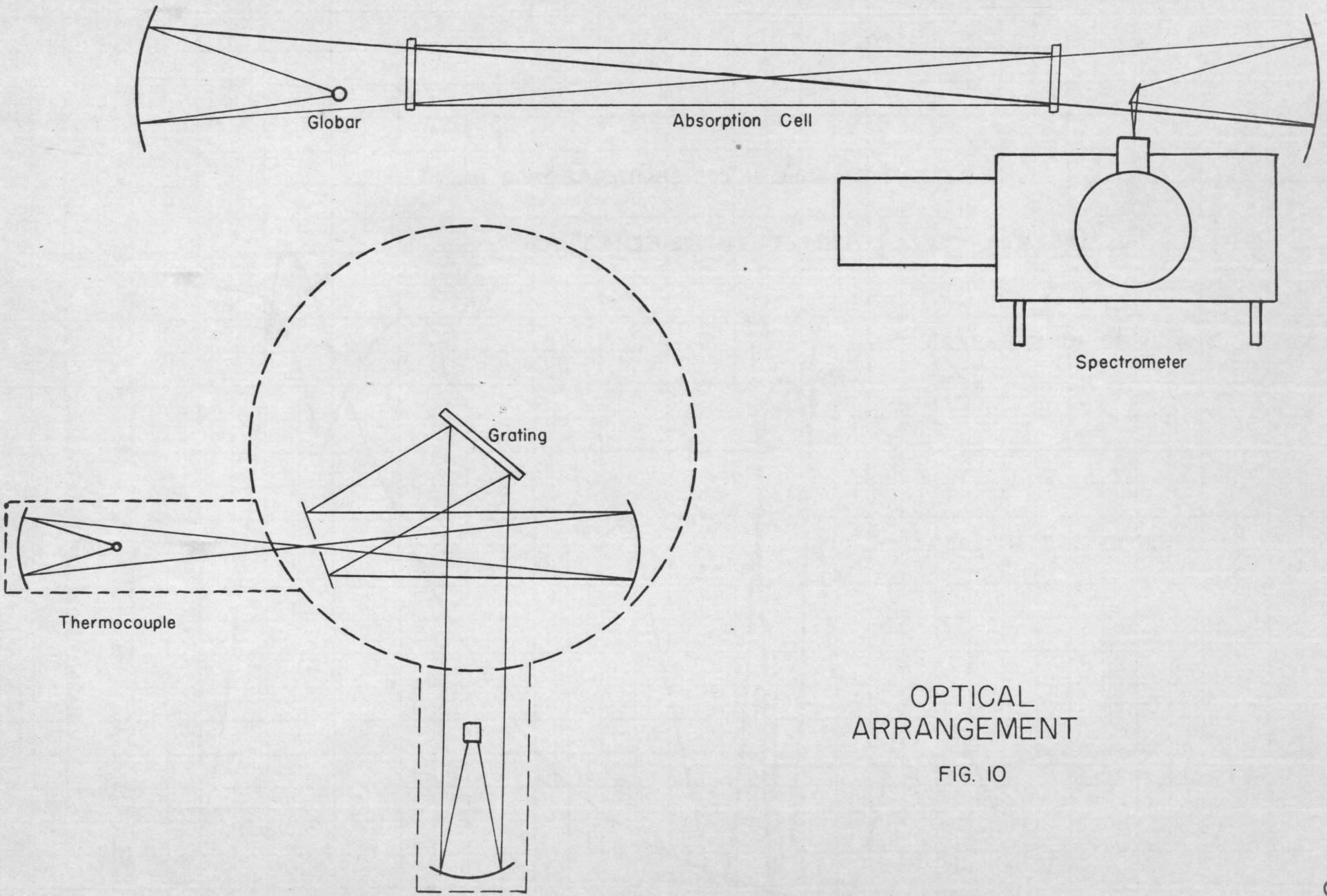

OPTICAL
ARRANGEMENT

FIG. 10

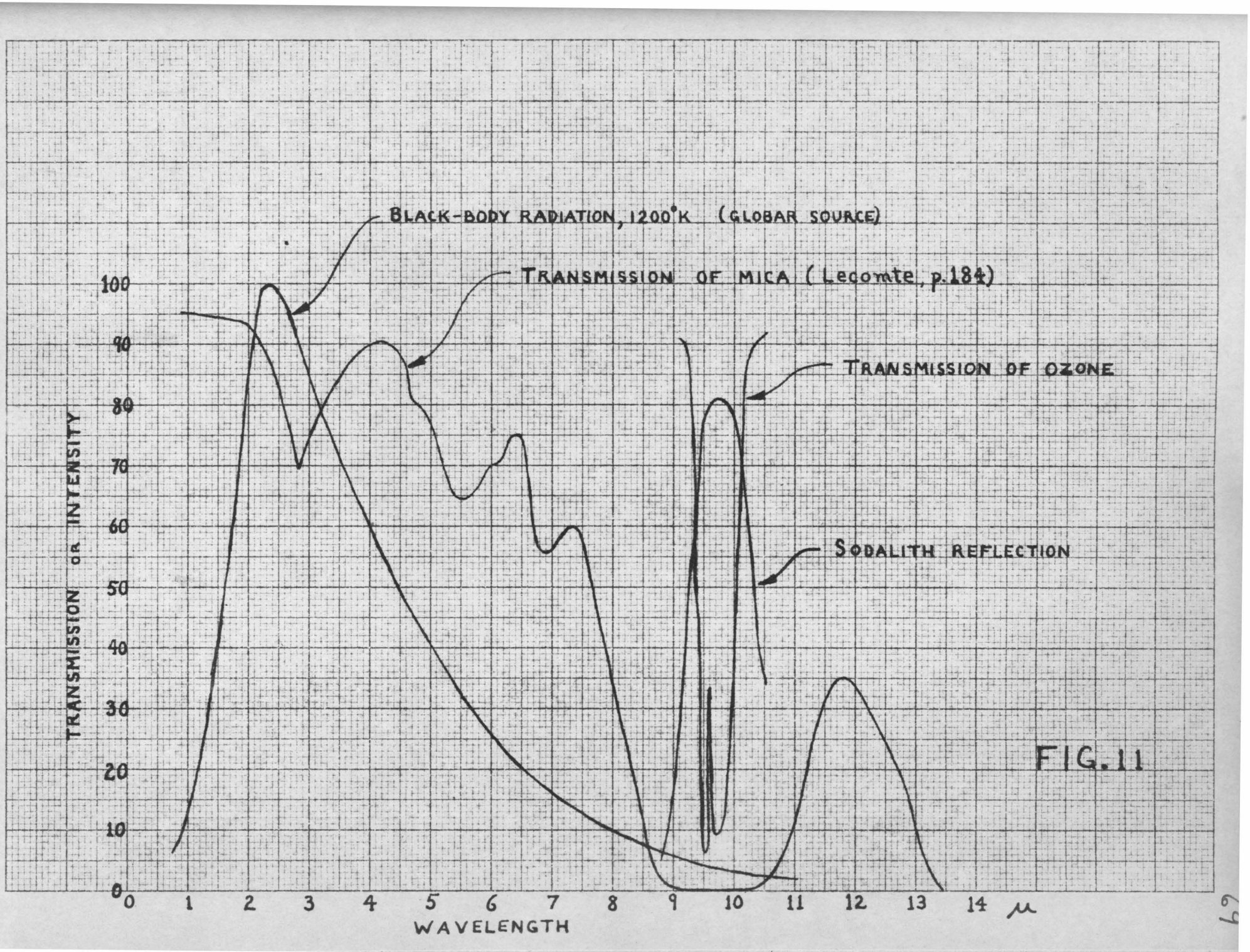
BLACK-BODY RADIATION, 1200°K (GLOBAR SOURCE)
TRANSMISSION OF MICA (Lecomte, p.184)
TRANSMISSION OF OZONE
SODALITH REFLECTION
TRANSMISSION OR INTENSITY
100
90
80
70
60
50
40
30
20
10
0
0 1 2 3 4 5 6 7 8 9 10 11 12 13 14 μ
WAVELENGTH

FIG. 11

FIG. 12

ABSORPTION AT 6 MM. PRESSURE

OZONE THICKNESSES:

1- 3.06 MM.
2- 2.31
3- 1.51
4- ~ 1.0 (faired in)
5- .42
6- .18

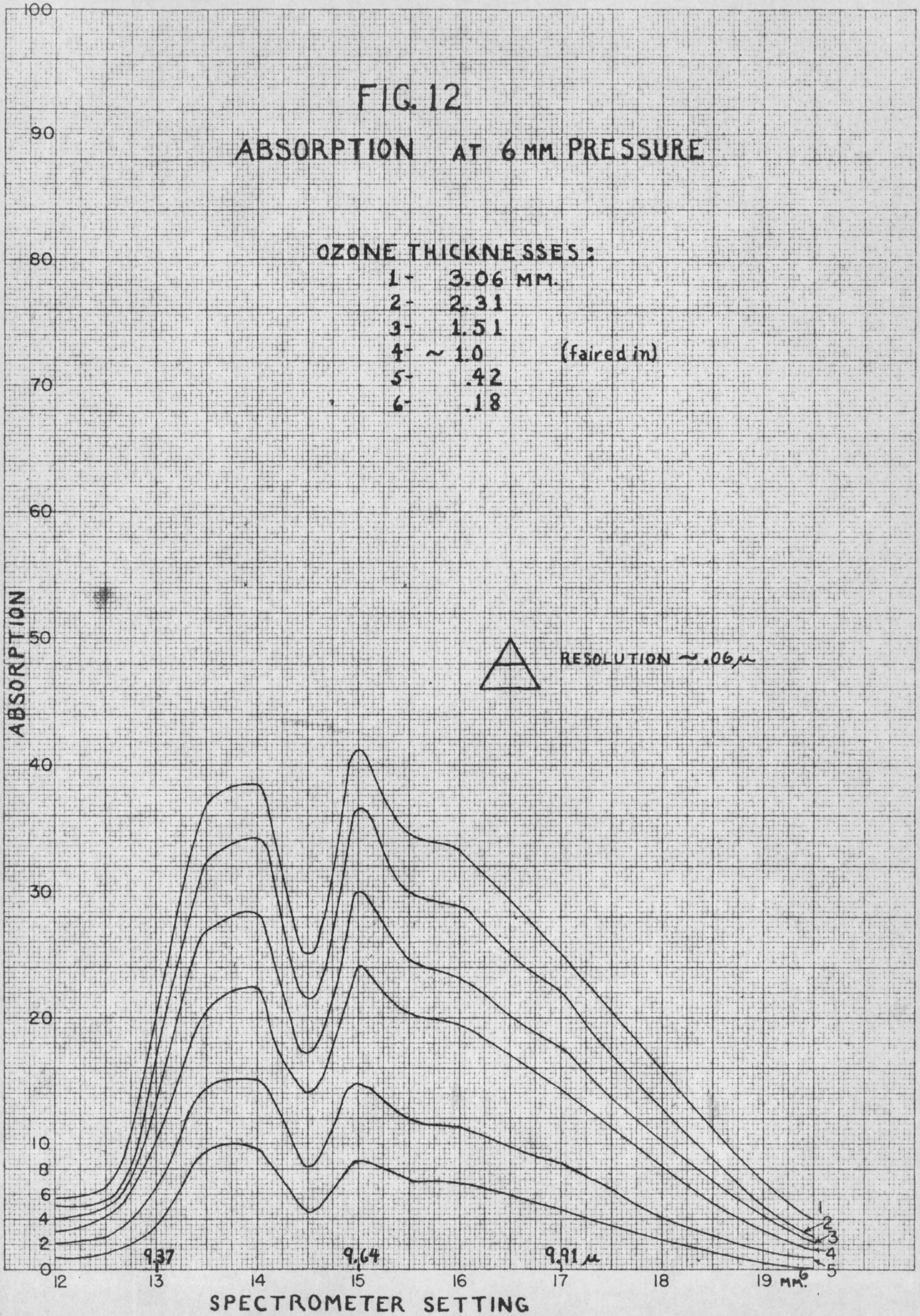

FIG. 13

ABSORPTION AT 13 MM. PRESSURE

OZONE THICKNESSES:
1 - 3.40 MM.
2 - 1.60
3 - .89
4 - .35
5 - .19

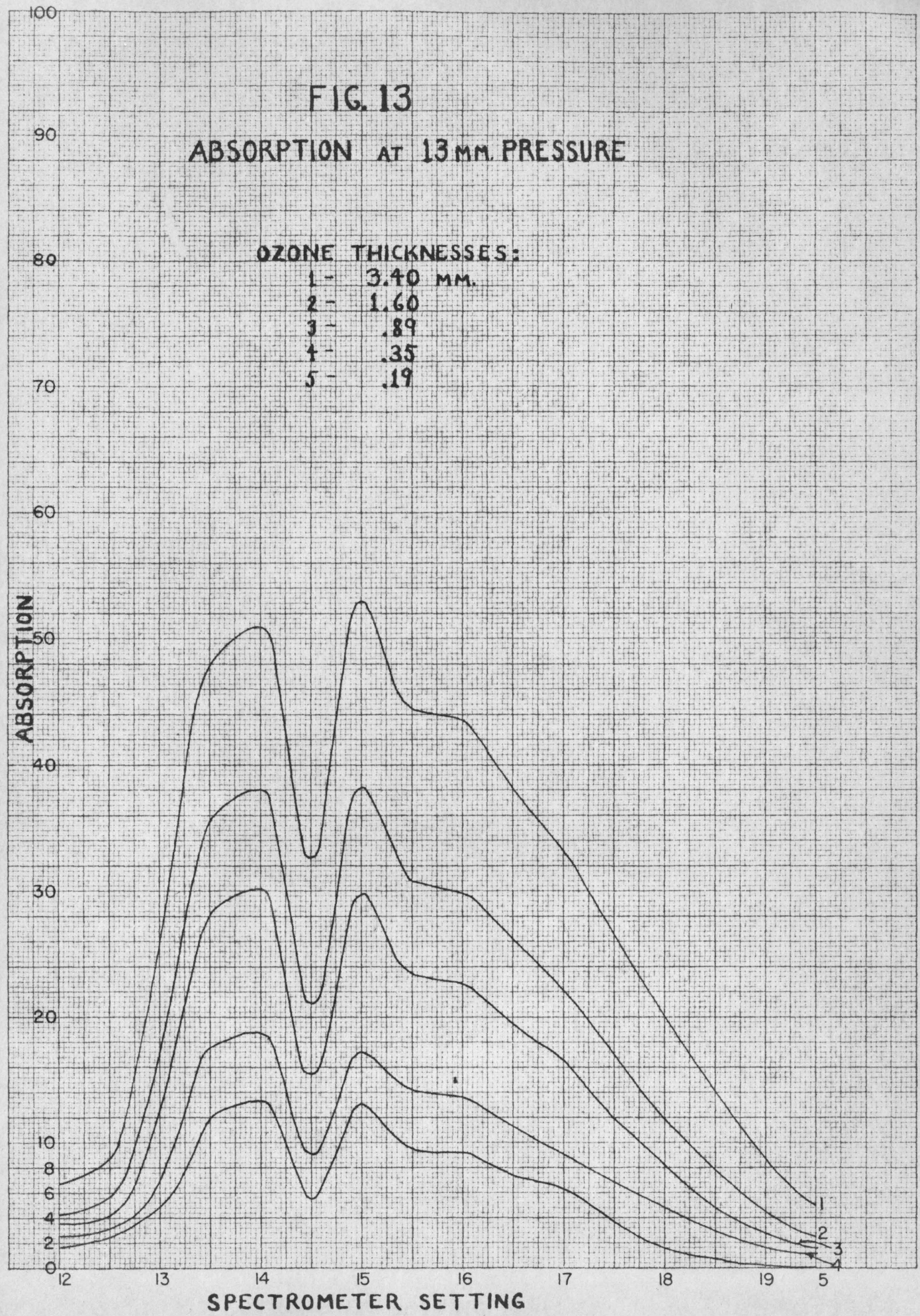

FIG. 14

ABSORPTION AT 25.8 MM. PRESSURE

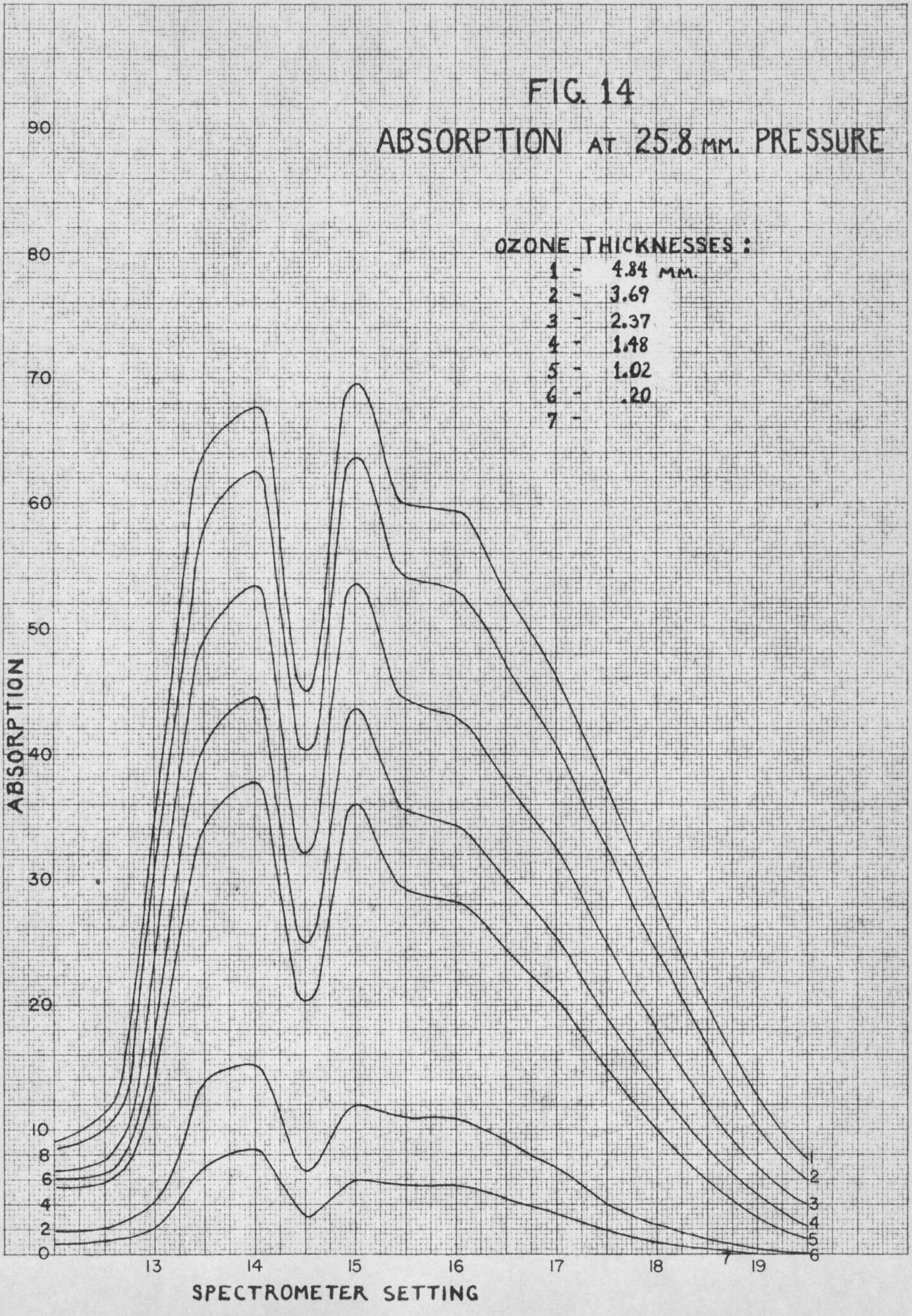

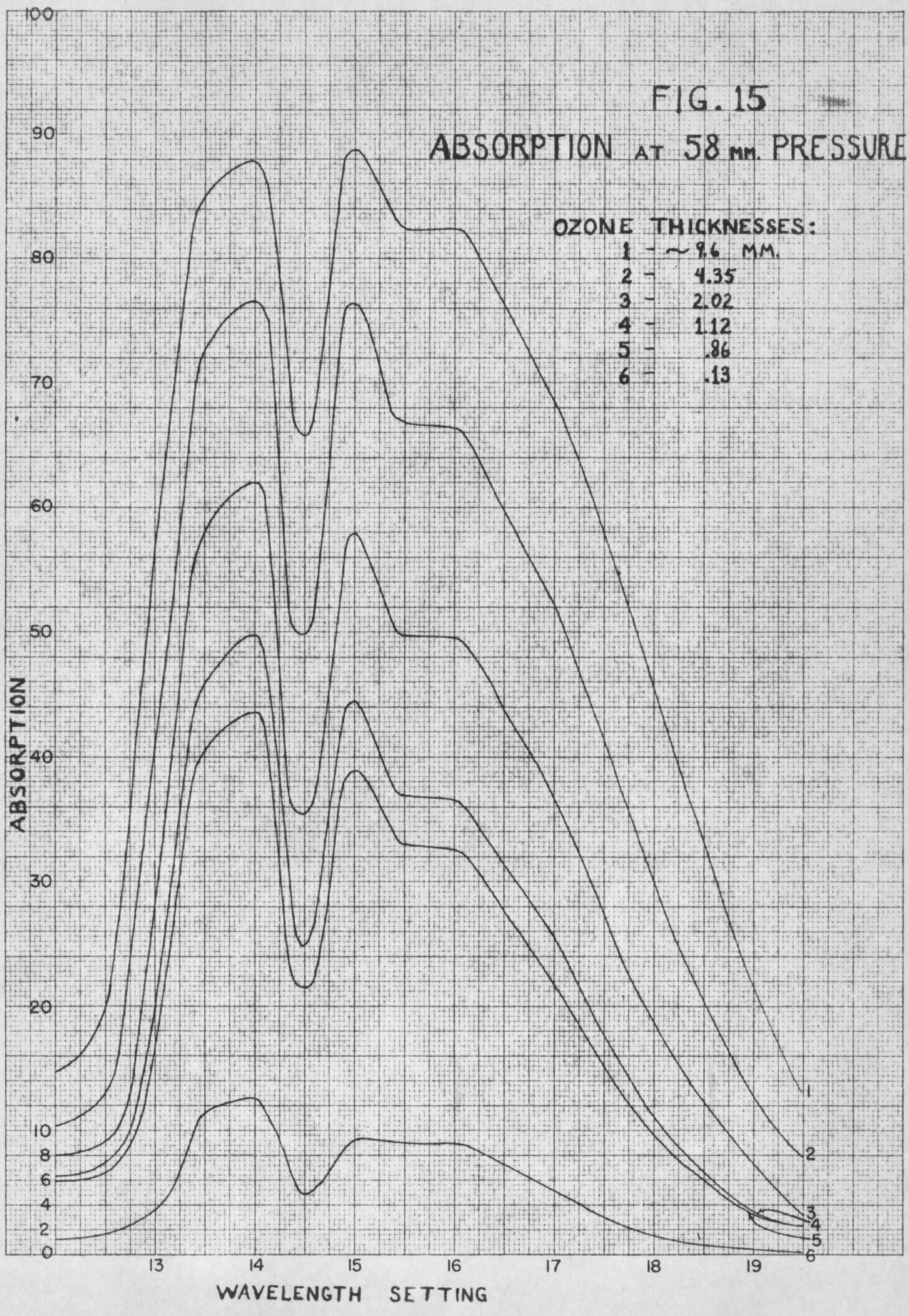
FIG. 15
ABSORPTION AT 58 MM. PRESSURE
OZONE THICKNESSES:
1 - ~9.6 MM.
2 - 4.35
3 - 2.02
4 - 1.12
5 - .86
6 - .13
ABSORPTION
WAVELENGTH SETTING
100
90
80
70
60
50
40
30
20
10
8
6
4
2
0
13
14
15
16
17
18
19
1
2
3
4
5
6

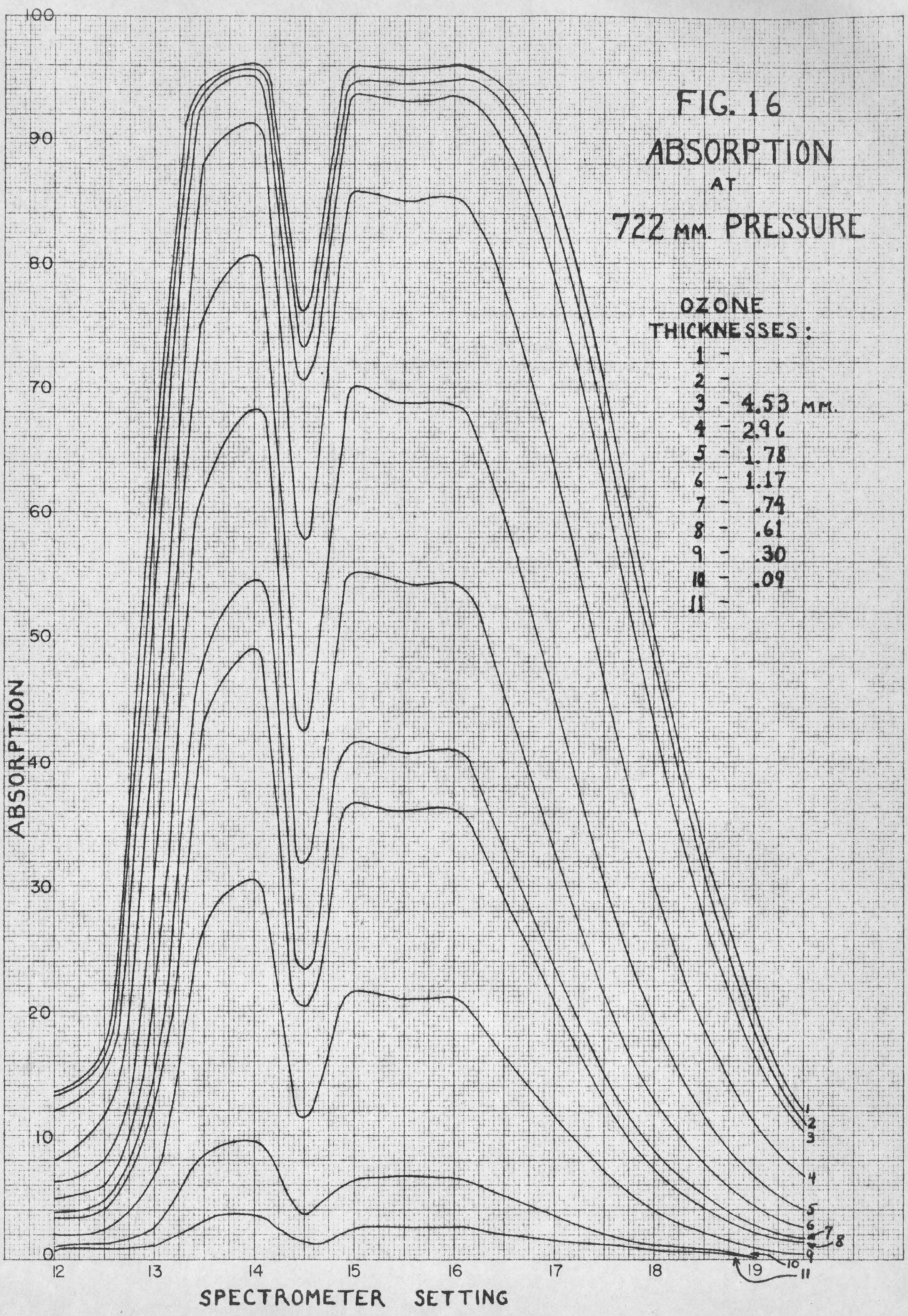
FIG. 16
ABSORPTION
AT
722 MM. PRESSURE
OZONE
THICKNESSES:
1 -
2 -
3 - 4.53 MM.
4 - 2.96
5 - 1.78
6 - 1.17
7 - .74
8 - .61
9 - .30
10 - .09
11 -
ABSORPTION
100
90
80
70
60
50
40
30
20
10
0
12
13
14
15
16
17
18
19
SPECTROMETER SETTING

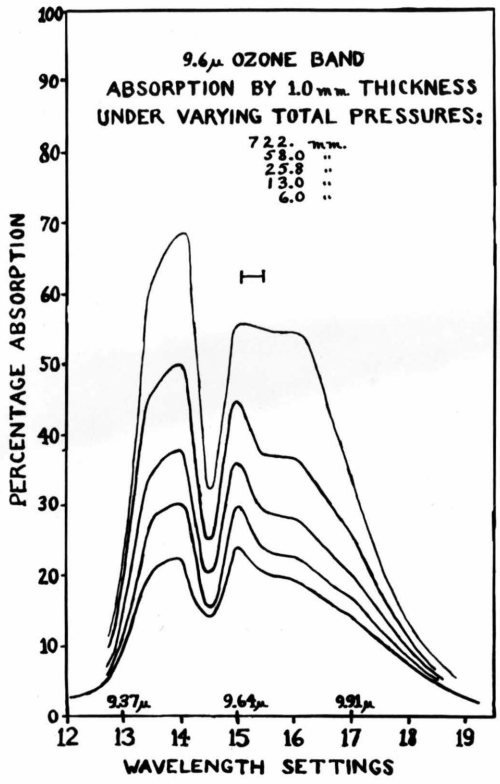
9.6μ OZONE BAND
ABSORPTION BY 1.0 mm. THICKNESS
UNDER VARYING TOTAL PRESSURES:
722. mm.
58.0 ".
25.8 ".
13.0 ".
6.0 ".
PERCENTAGE ABSORPTION
100
90
80
70
60
50
40
30
20
10
0
9.37μ
9.64μ
9.91μ
12
13
14
15
16
17
18
19
WAVELENGTH SETTINGS

FIG. 17

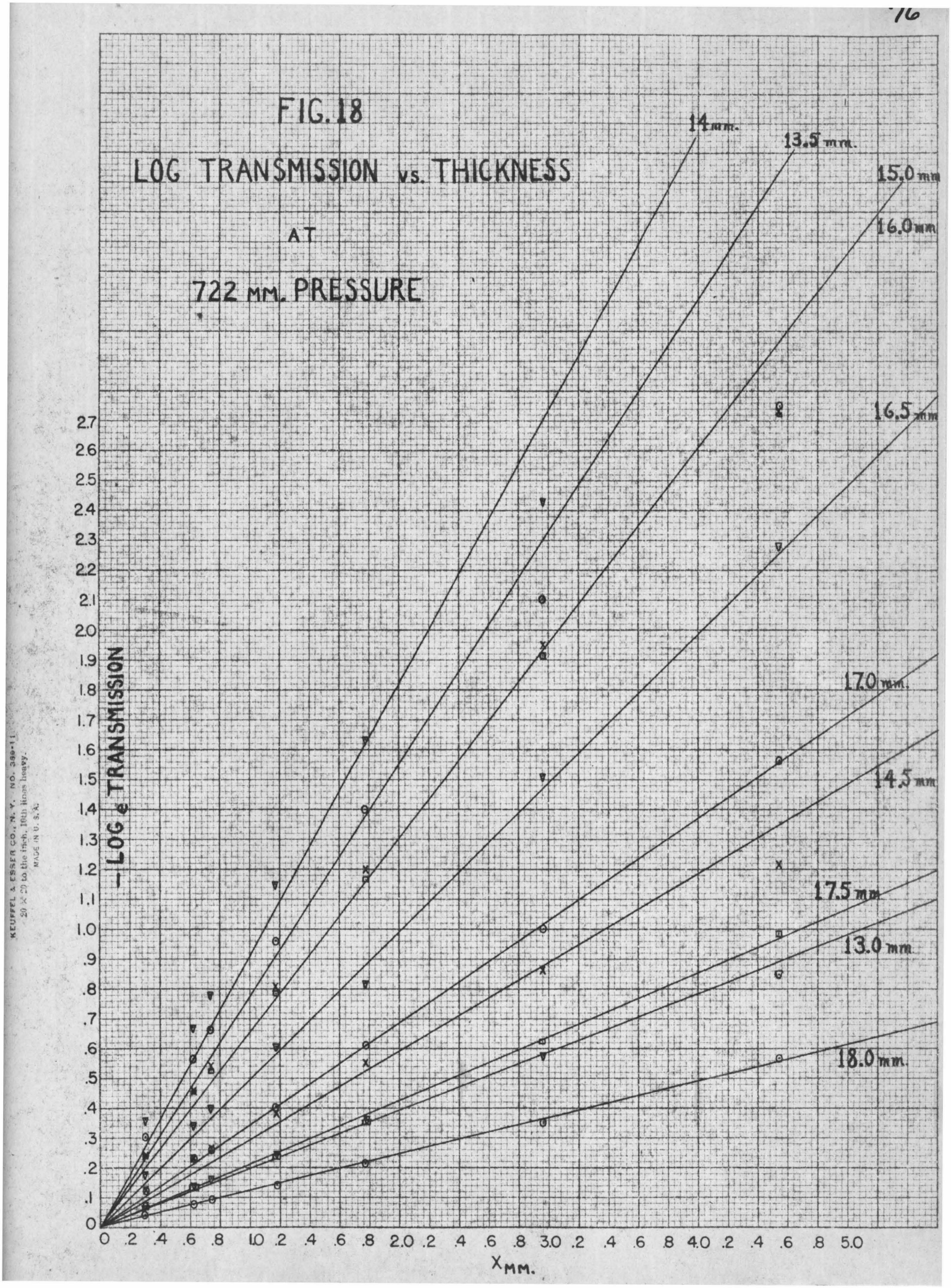
FIG. 18
LOG TRANSMISSION vs. THICKNESS
AT
722 MM. PRESSURE
14 mm.
13.5 mm.
15.0 mm
16.0 mm
16.5 mm
17.0 mm.
14.5 mm
17.5 mm
13.0 mm
18.0 mm.
-LOG e TRANSMISSION
X MM.
0 .2 .4 .6 .8 1.0 .2 .4 .6 .8 2.0 .2 .4 .6 .8 3.0 .2 .4 .6 .8 4.0 .2 .4 .6 .8 5.0
0 .1 .2 .3 .4 .5 .6 .7 .8 .9 1.0 1.1 1.2 1.3 1.4 1.5 1.6 1.7 1.8 1.9 2.0 2.1 2.2 2.3 2.4 2.5 2.6 2.7
KEUFFEL & ESSER CO., N. Y. NO. 358-11
20 × 20 to the inch. 10th inch heavy.
MADE IN U. S. A.

FIG. 19

LOG TRANSMISSION vs. THICKNESS

AT

58 MM. PRESSURE

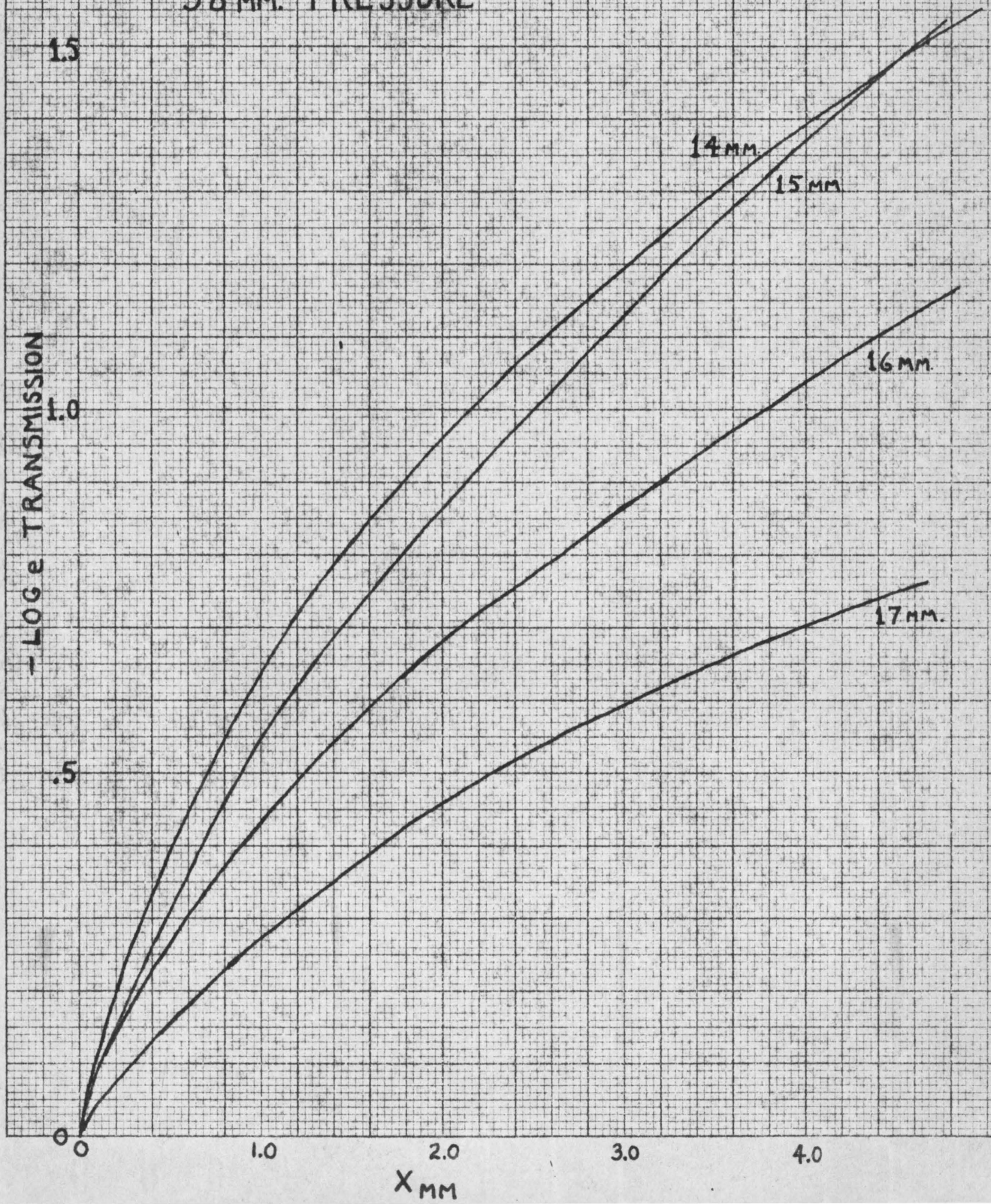

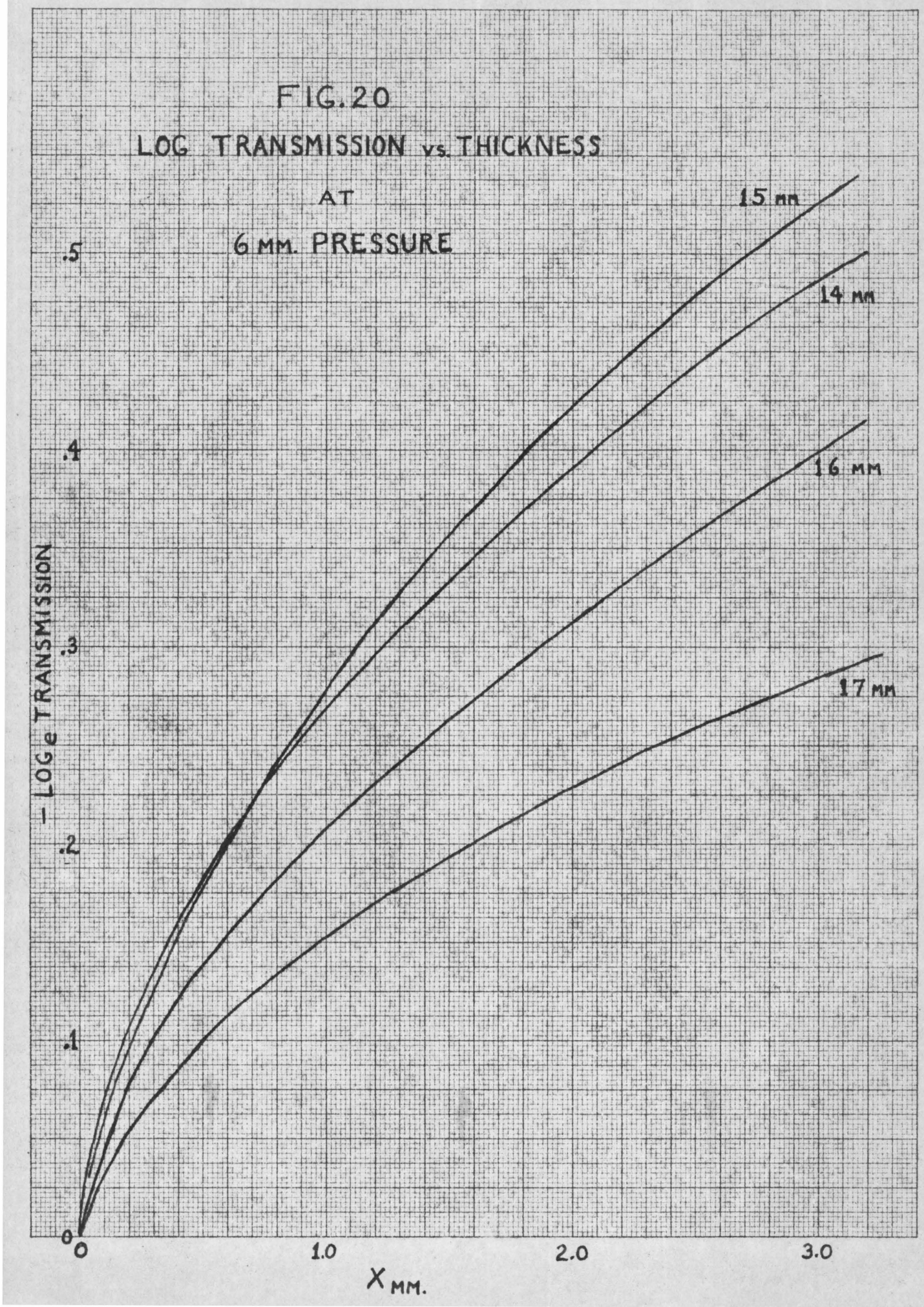
FIG. 20
LOG TRANSMISSION vs. THICKNESS
AT
6 MM. PRESSURE
15 MM
14 MM
16 MM
17 MM
.5
.4
.3
.2
.1
0
0
1.0
2.0
3.0
X MM.
- LOG e TRANSMISSION

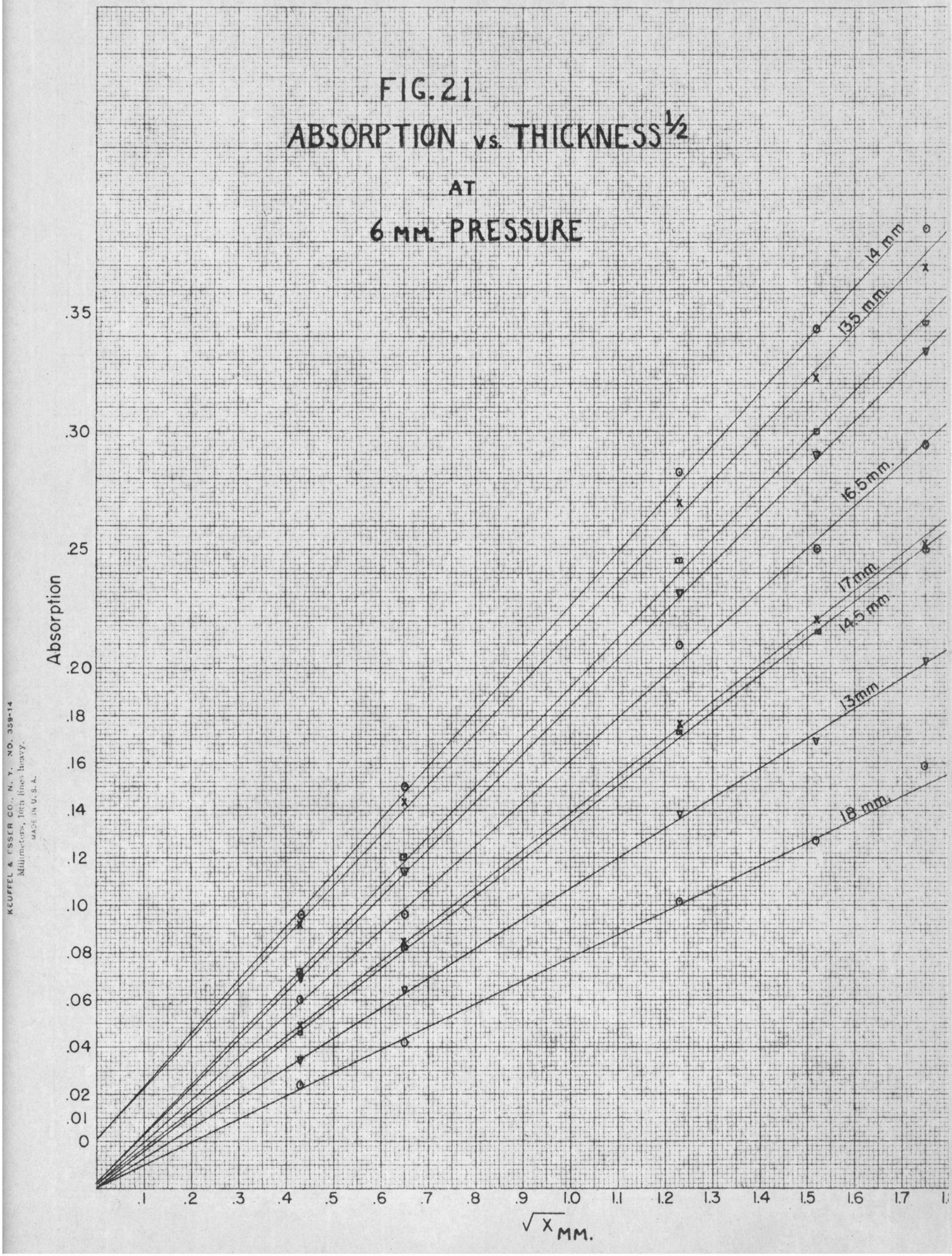

FIG. 22

ABSORPTION vs. THICKNESS$^{1/2}$

AT

58 MM. PRESSURE

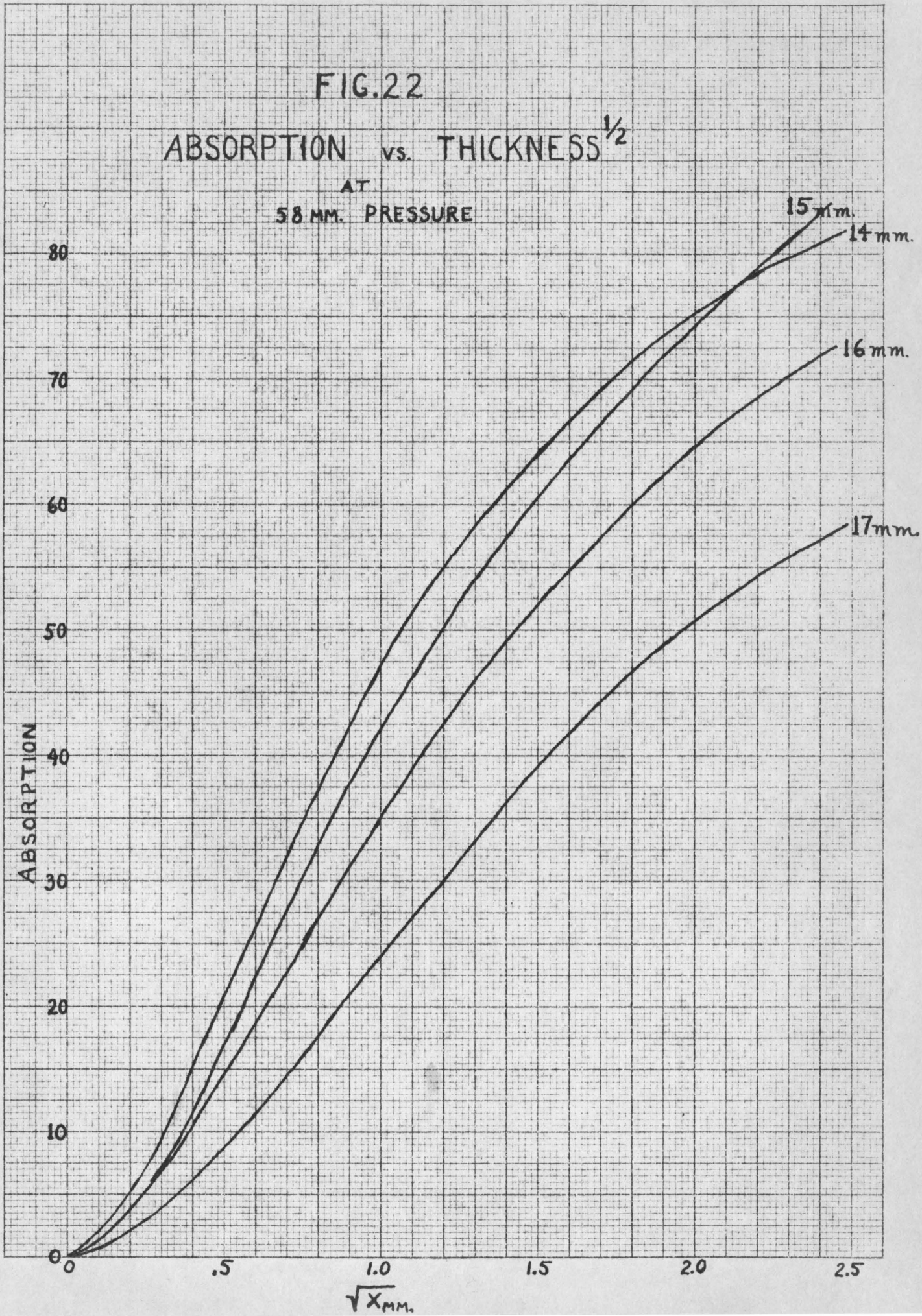

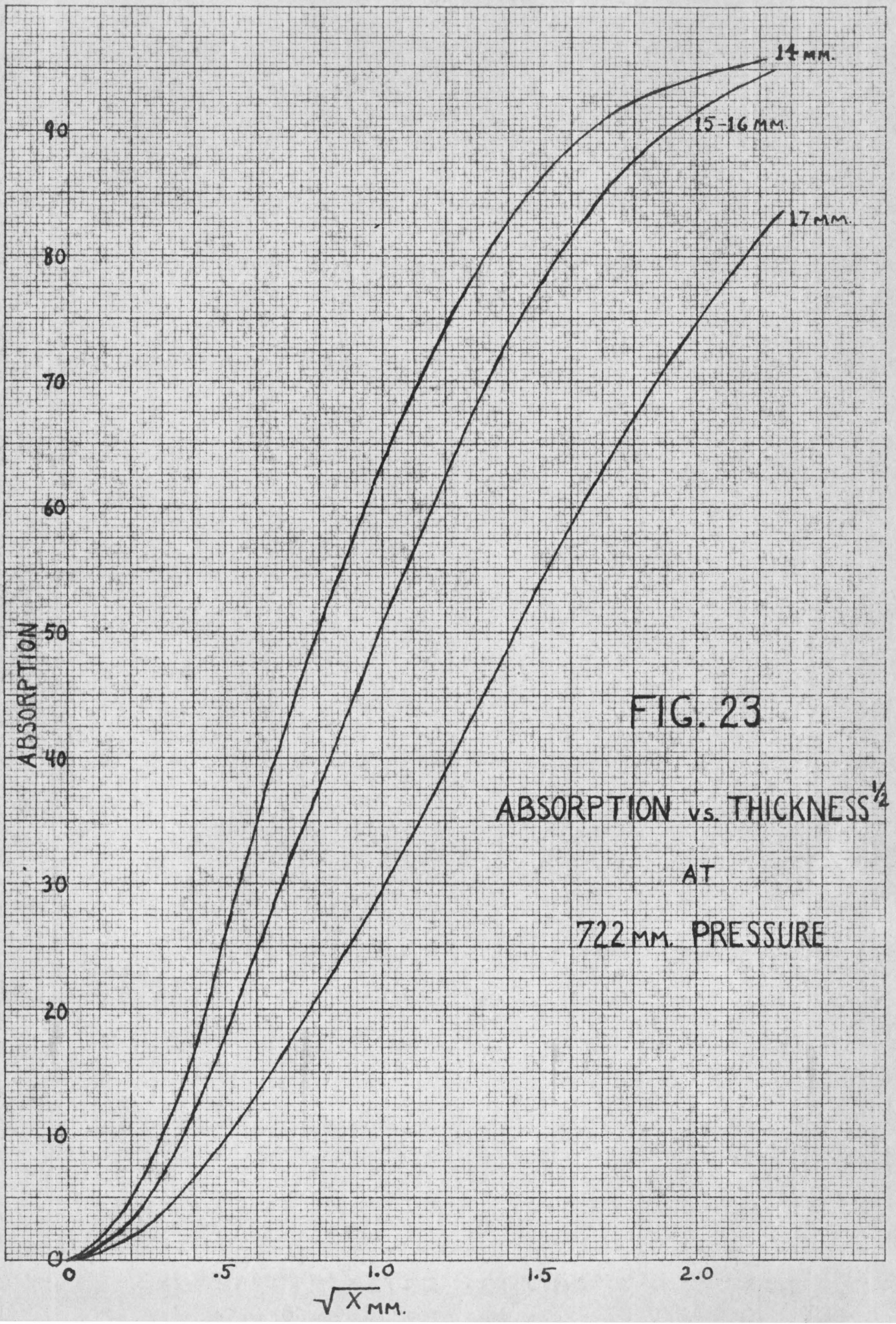

FIG. 23

ABSORPTION vs. THICKNESS$^{1/2}$

AT

722 mm. PRESSURE

FIG. 24

DENSITY CONTOUR OF 9.6 μ BAND OF OZONE

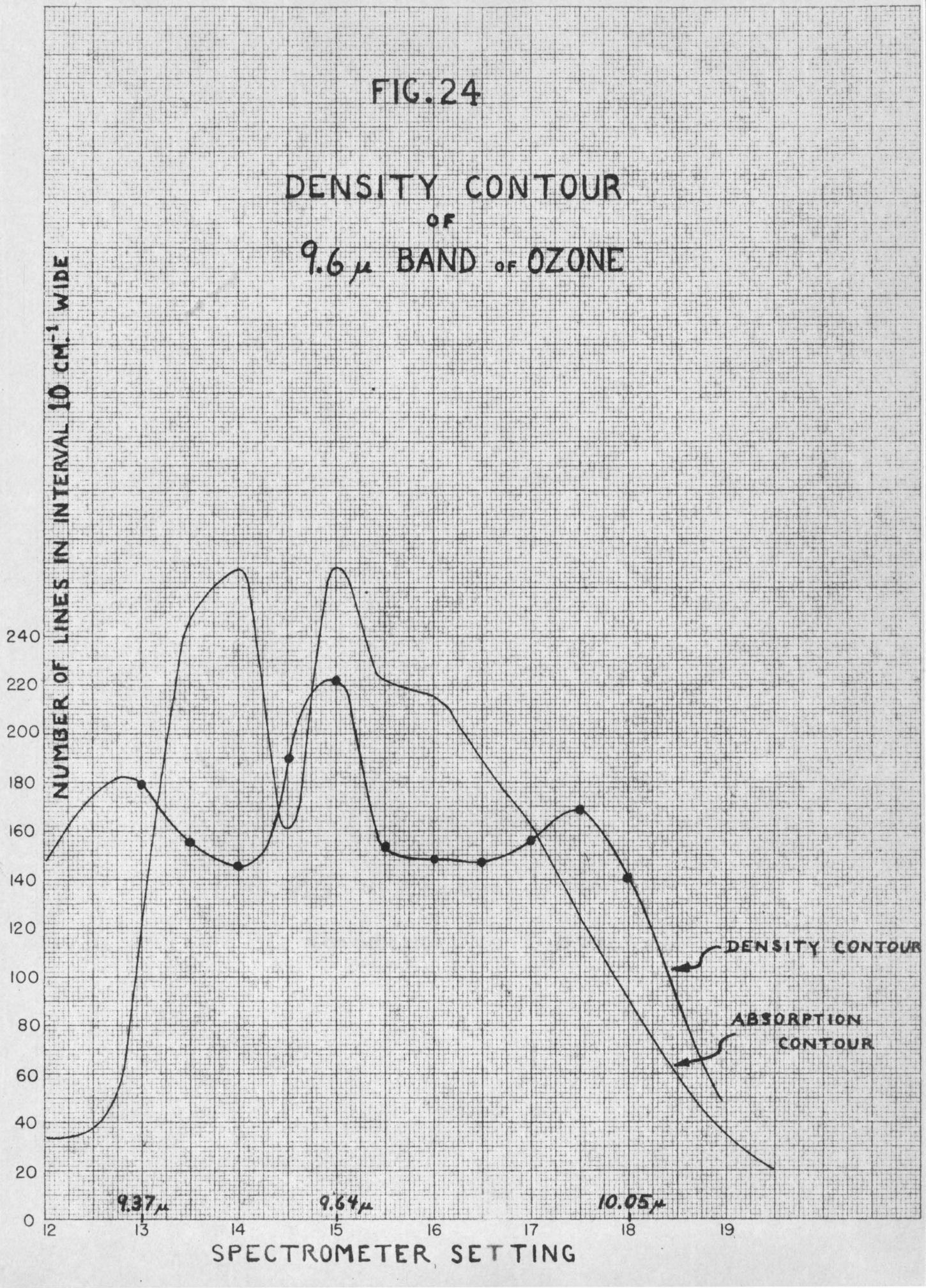

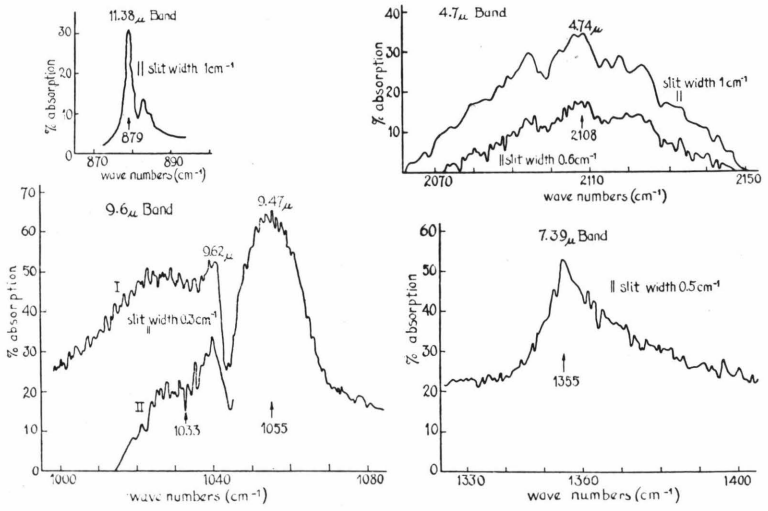

FIG. 25 – OZONE SPECTRUM, ACCORDING TO GERHARD.

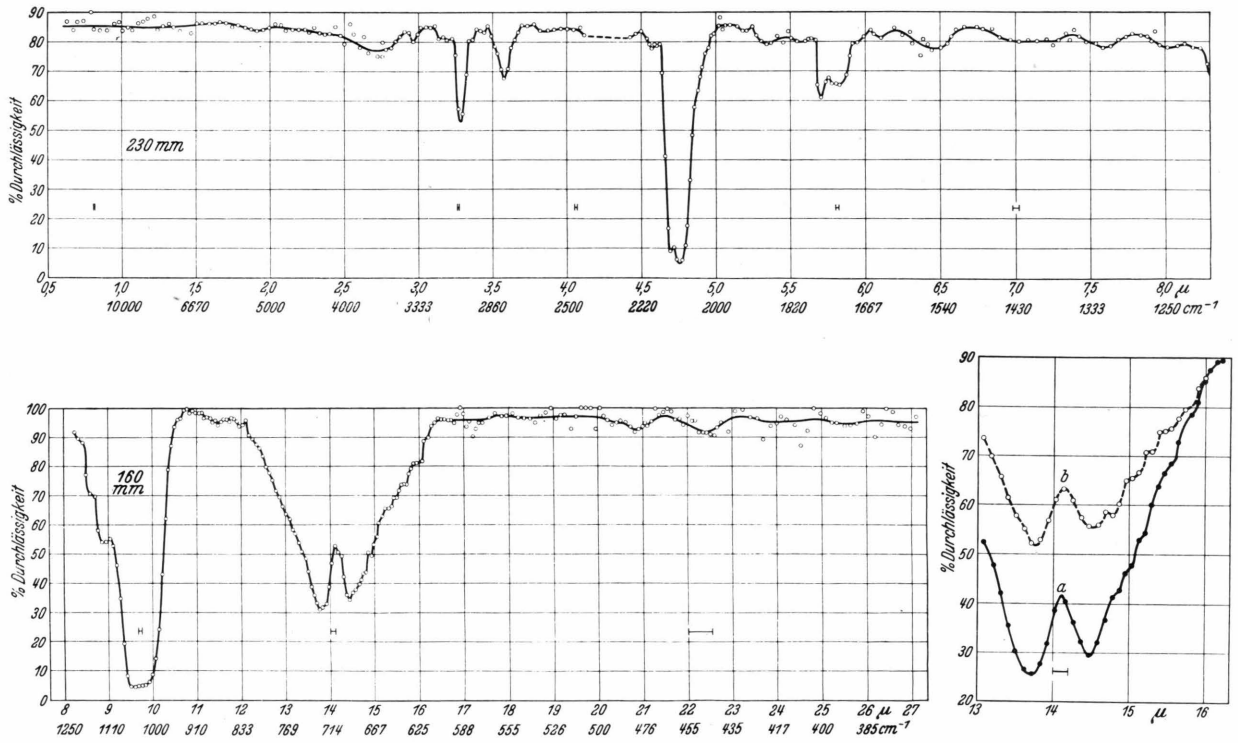

FIG. 26 — OZONE SPECTRUM, ACCORDING TO HETTNER, POHLMAN, SCHUMACHER

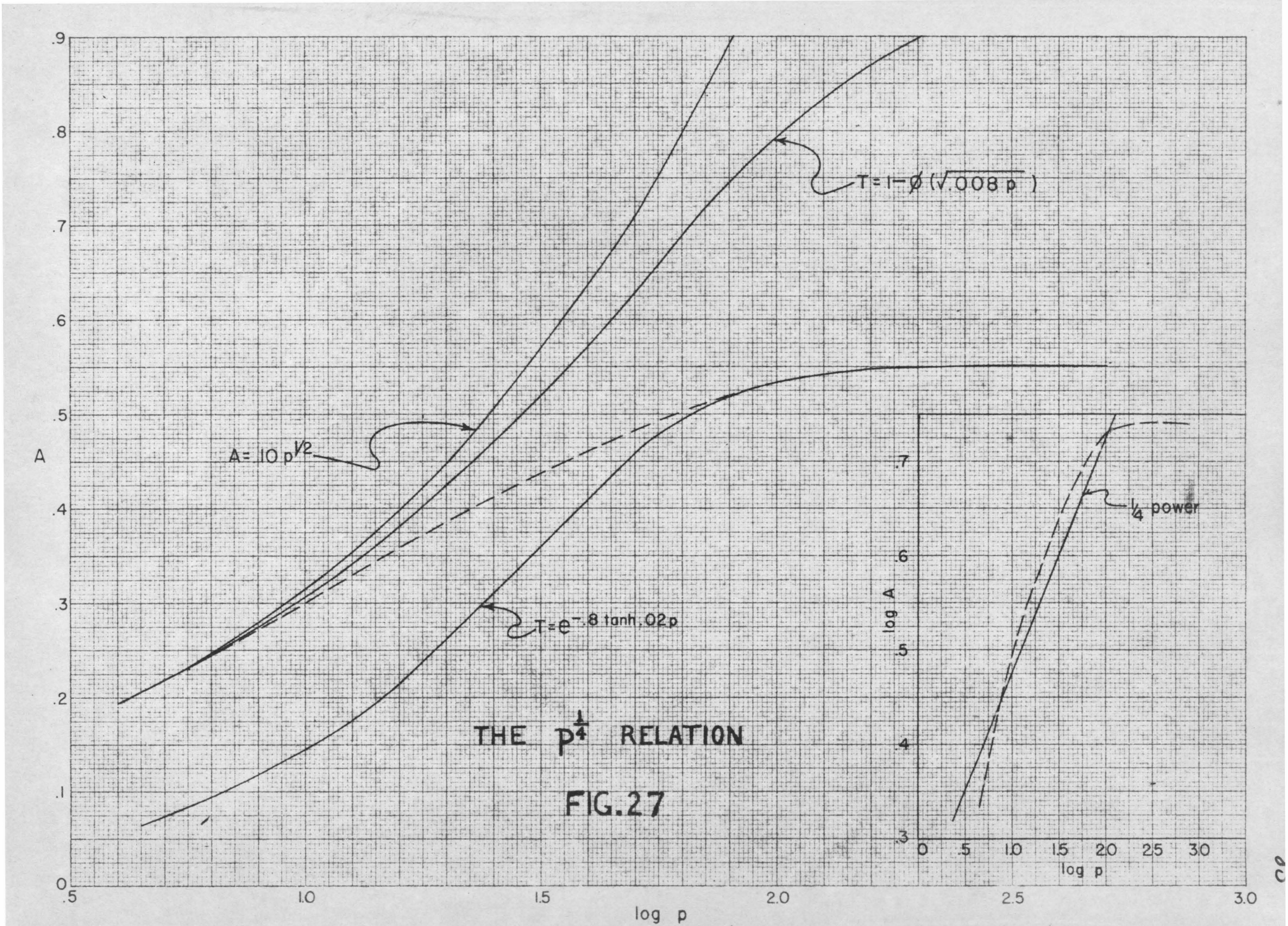

THE $p^{\frac{1}{4}}$ RELATION

FIG. 27

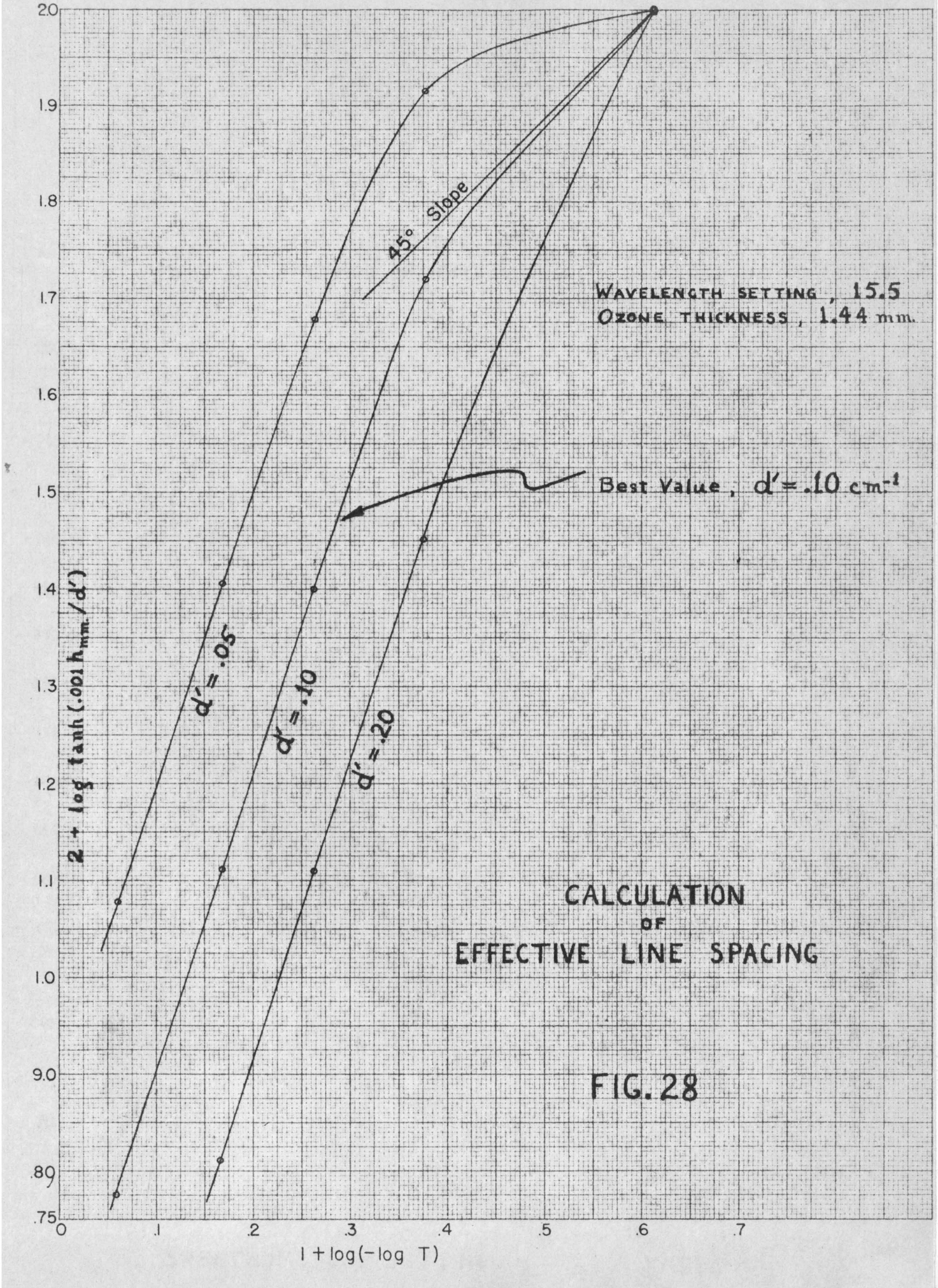

CALCULATION
OF
EFFECTIVE LINE SPACING

FIG. 28

FIG. 29

DENSITY CONTOUR

USING THE
METHOD OF APPENDIX F

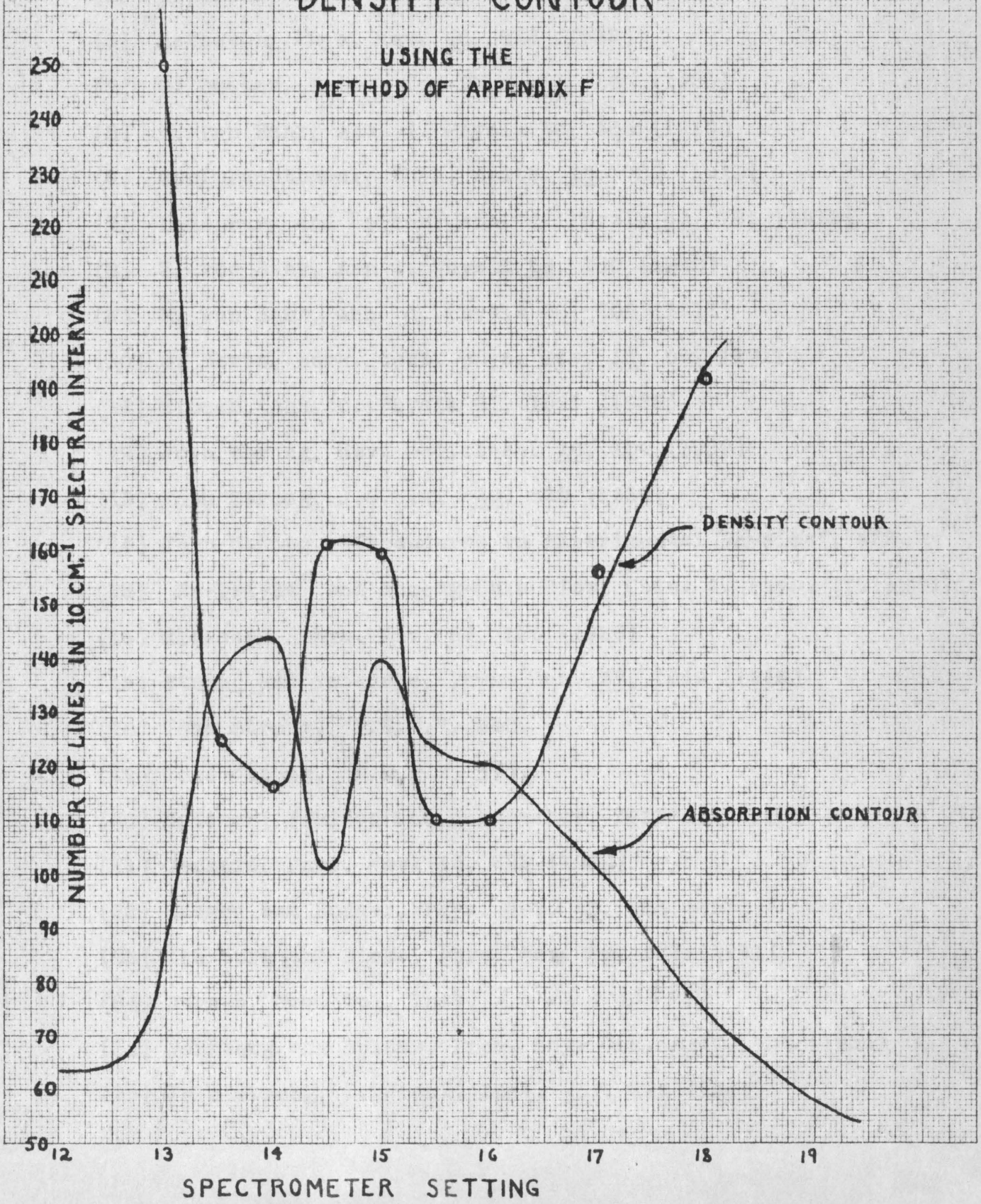

REFERENCES

(1) Margenau and Watson, Rev. Mod. Phys. 8, 22 (1936)

(2) Elsasser, Astro. J. 87, 497 (1938)

(3) Matheson, Phys. Rev. 40, 813 (1932)

(4) G. Becker, Zeits. fur Phys. 34, 255 (1926)

(5) E. von Bahr, Ann. d. Physik 33, 585 (1910)

(6) Chr. Fuchtbauer, Phys. Zeits. 12, 722 (1911)

(7) Ladenburg and Reiche, Ann. d. Physik 42, 181 (1913)

(8) E. von Bahr, Ann d. Physik 29, 780 (1909)

(9) E. von Bahr, Ann. d. Physik 38, 206 (1912)

(10) G. Hertz, Verh. deut. phys. Ges. 13, 617 (1911)

(11) Wimmer, Ann. d. Physik 81, 1091 (1926)

(12) John Strong, Rev. Sci. Inst. 10, 104 (1939)

(13) John Strong, J.O.S.A. 29, 520 (1939(

(14) John Strong, "Procedures in Experimental Physics", 422.

(15) Ny-Tsi-Ze' and Choong-Shin-Piaw, Chin. J. Phys. 1,1(1933)

(16) Elsasser, Phys. Rev. 54, 126 (1938)

(17) Strong and Watanabe, Phys. Rev. 57, 1049 (1940)

(18) John Strong, "P.E.P.", 348.

(19) John Strong, "P.E.P.", 379.

(20) Hettner, Pohlman and Schumacher, Zeits. fur Phys. 91,372 (1934)

(21) Gerhard, Phys. Rev. 42, 622 (1932)

(22) Badger and Bonner, Phys. Rev. 43, 305 (1933)

(23) Ginsburg and Dieke, Phys. Rev. 59, 632 (1941)

(24) Barnes, Rev. Sci. Inst. 7, 265 (1936)

(25) Herzberg and Spinks, Proc. Roy. Soc. A147, 434 (1934)

(26) John Strong, J. Frank. Inst. 231, 121 (1941)